Polar bear (*Ursus maritimus*) use of the western Hudson Bay flaw lead

by

Erin McKenzie Henderson

A thesis submitted in partial fulfillment of the requirements for the degree of

Master of Science

in

Ecology

Department of Biological Sciences
University of Alberta

ABSTRACT

Polynyas and leads are recurrent areas of open water within sea ice that are important to many Arctic species, including marine mammals; however, the importance to polar bears (*Ursus maritimus*) has not been examined. The western Hudson Bay flaw lead (hereafter lead) is a major, predictable habitat feature within the home range of the Western Hudson Bay polar bear population. The lead may provide hunting opportunities, but equally, could represent barriers to movement. We assessed use of the lead by 73 adult female polar bears tracked using satellite telemetry from December 2009 – May 2018 by measuring 1) distance to the lead, 2) movement direction relative to the lead, 3) first passage time, 4) turning angles, and 5) crossing rate of the lead. The use of the lead was compared 1) temporally, 2) spatially, and 3) based on reproductive status. The lead was mapped using synthetic aperture radar (resolution 62.3 m x 121 m) to differentiate between ice and water in Hudson Bay. The width of the lead varied temporally, from 4.5 km in March, up to 145 km in May. Polar bear use of the lead varied temporally, spatially, and based on reproductive status. Polar bears were closest to the lead in May during seal pupping season when polar bears are hyperphagic, and furthest from the lead in December. Polar bears had faster, more directed movements along the lead (moving on average with 16° turning angles at 101° and -69° relative to the feature) when closer to narrower sections of the feature, suggesting the feature acts as a corridor to increase prey encounter rate. Bears were consistently closer to narrow sections of the lead, and females with cub(s)-of-the-year were on the narrowest sections. Furthermore, while the bears crossed the lead 50% of the time overall, crossings occurred more often in January – March (80% of crossings) than in April or May (39%) when the feature was less prominent. These results suggest that a wider lead might deter crossings and restrict bear movements, particularly for mothers with cub(s)-of-the-year. When

females of all reproductive classes were ≤1 median step length from the lead, however, lone females spent more time close to the lead than mothers with cub(s)-of-the-year and yearling(s). Prey likely attracts polar bears to the lead, but bears might limit their time in the area because of the higher energetic costs of travelling in unconsolidated ice and retreat to habitat further from the lead between hunts to conserve energy. Furthermore, mothers with cub(s)-of-the-year might limit their time on the lead to reduce the risk of infanticide by males that are attracted to areas with lone females for mating purposes, or because of prey availability. An increase in open water resulting from climate warming might make the lead a more challenging environment for bears, yet possibly more attractive as the spring feeding period decreases and energy intake declines, or as harbour seal density increases in the area.

PREFACE

This thesis is an original work by Erin McKenzie Henderson. Synthetic aperture radar data used to generate the flaw lead maps were compiled and provided by Dr. B. Montpetit at the National Wildlife Research Centre. Global positioning system collars deployed by Dr. A. E. Derocher and Dr. N. J. Lunn at the University of Alberta and Environment and Climate Change Canada, respectively, provided data on polar bear movements for this research. I acknowledge the use of imagery from the NASA Worldview application (*https://worldview.earthdata.nasa.gov/*), part of the NASA Earth Observing System Data and Information System (EOSDIS).

To date, the manuscript has not been submitted to a peer-reviewed journal. Dr. A. E. Derocher, Dr. N. J. Lunn, Dr. E. S. Richardson, Dr. B. Montpetit, and Dr. E. H. Merrill provided valuable feedback and edits throughout the analysis and writing processes.

Animal capture and handling procedures received research ethics approval from the University of Alberta BioSciences Animal Care and Use Committee, project name “Polar Bears and Climate Change: Habitat Use and Trophic Interactions”, No. AUP00000033.

ACKNOWLEDGEMENTS

I would like to thank Dr. A. E. Derocher for welcoming me into his lab, for his support and direction with the research, his dedication to the review of numerous drafts, his academic guidance, and financial support he has provided. I thank Dr. E. S. Richardson for bringing Dr. B. Montpetit into the project to help with the ice imagery, and for his review of results and drafts of the thesis. I thank Dr. B. Montpetit for the time and effort he put in to analyse the raw satellite imagery, and for his guidance with my subsequent analysis. I thank Dr. E. H. Merrill for her guidance regarding the statistical analysis, and Dr. N. J. Lunn for his review of results. I thank David McGeachy for providing me with data to further my analyses. I thank Ron Togunov, Amy Johnson, Peter Thompson, and Alyssa Bohart for their support and guidance for parts of the analysis, and for reading drafts of the thesis. I thank my friends in the Derocher lab for their support and encouragement throughout grad school. I would like to thank my parents, grandparents, and sister, who have supported me throughout my education.

Funding and logistical support for this project was provided by the Churchill Northern Studies Centre, Environment and Climate Change Canada, Natural Sciences and Engineering Research Council of Canada, University of Alberta, Earth Rangers, Hauser Bears, Isdell Family Foundation, Parks Canada Agency, Polar Bears International, Quark Expeditions, The Ocean Foundation, the Schad Foundation, Wildlife Media, Inc., and World Wildlife Fund Canada.

TABLE OF CONTENTS

LIST OF TABLES

LIST OF FIGURES

CHAPTER 1

INTRODUCTION

Arctic sea ice provides habitat for a wide range of species, from single-celled organisms to top predators, living under, within, and on the sea ice (Smith & Stirling 1975, Horner et al. 1992, Poltermann 2001, David et al. 2016, Hammill 2018). The Arctic is a dynamic habitat, with areas covered by sea ice year-round, producing a thick multiyear buildup of ice, and areas that melt each year, characterized by thinner annual ice (Horner et al. 1992, Laxon et al. 2003, Comiso 2010). Sea ice extent varies seasonally, decreasing by over half at the minimum, with high spatial variation in thickness (Laxon et al. 2003, Comiso 2010, Landy et al. 2017). There are different types and characteristics of sea ice that make it suitable habitat for a wide range of species. Landfast ice is stable ice that extends from the coastline to a variable distance offshore that is largely dependent on ocean depth (Comiso 2010). Adjacent to the landfast ice is a more dynamic environment of drifting pack ice, which can be consolidated ice sheets, or comprised of small and/or large ice floes separated by water, and driven together or apart by winds/currents (Smith et al. 1990, Horner et al. 1992, Comiso 2010). Ice can open up into recurring, persistent features of open water called polynyas, or smaller, linear leads (Danielson 1971, Dunbar 1981, Barber & Massom 2007).

Polynyas and recurring lead systems have a circumpolar distribution, occurring over both continental shelf and offshore waters, and ranging in size from 10 to 10^5 km^2 (Martin 2001, Barber & Massom 2007, Hannah et al. 2009). There are 61 major, recurring polynyas across the Arctic, 23 of which are in the Canadian Arctic (Barber & Massom 2007, Hannah et al. 2009). Open water that forms between pack ice and fast ice, or pack ice and the shore, are flaw leads or shore leads, respectively, and are more dynamic than other areas in the Arctic (Stirling 1980,

Dunbar 1981, Smith & Rigby 1981, Barber & Massom 2007). Winds, currents, tides, and/or upwellings are the primary causes of polynyas and leads, and make them dynamic icescape features that vary in size and shape (Stirling 1980, Dunbar 1981, Stirling 1981, Barber & Massom 2007, Hannah et al. 2009). Pack ice can be driven towards fast ice to close polynyas, driven away from fast ice making polynyas completely ice free, or brash/thin ice can form within open polynyas as they refreeze (Hare & Montgomery 1949, Stirling 1980, Dunbar 1981, Smith & Rigby 1981, Barber & Massom 2007). Polynyas and leads typically reform annually in the same location, resulting in predictable habitat features important for organisms on the icescape (Stirling 1980, Smith & Rigby 1981, Stirling 1981, Heide-Jørgensen et al. 2013).

Biodiversity is often higher in polynyas compared to other Arctic areas due to the availability of open water (Stirling 1980, Arrigo 2007, Heide-Jørgensen et al. 2013, 2016). While sympagic algae are a large contributor of carbon to higher trophic levels in the Arctic, areas with lower ice cover, such as polynyas, are more reliant on pelagic algae for primary production (Mei et al. 2003, Arrigo & van Dijken 2004, Brown et al. 2013, 2018). Open water increases sunlight and surface temperatures compared to the surrounding ice pack, which promotes earlier primary production, allowing for higher zooplankton diversity (Bursa 1963, Hirche et al. 1991, Ringuette et al. 2002, Tremblay et al. 2002, Arrigo 2007). Increased primary and secondary production supports higher trophic level organisms, such as seabirds and marine mammals (Stirling et al. 1981, Karnovsky et al. 2007, 2008). Polynyas are important breeding and staging habitat for some seabirds (Brown & Nettleship 1981, Falk et al. 1997, Black et al. 2012). Similarly, Arctic marine mammals such as bearded seals (*Erignathus barbatus*), ringed seals (*Pusa hispida*), harbour seals (*Phoca vitulina*), walrus (*Odobenus rosmarus*), beluga whales (*Delphinapterus leucas*), narwhals (*Monodon monoceros*), and bowhead whales (*Balaena mysticetus*) are

abundant in polynyas and leads, which provide habitat for feeding, breeding, breathing, and migrating (Stirling et al. 1981, Gilchrist & Robertson 2000, Bajzak et al. 2013, Heide-Jørgensen et al. 2013, 2016). Polynyas are thought to be prime hunting habitat for upper trophic level predators, such as polar bears, due to the abundance and accessibility of prey (Stirling 1980, Heide-Jørgensen et al. 2013).

Polar bears (*Ursus maritimus*) rely on Arctic sea ice for hunting, mating, and travelling (Lentfer 1972, Stirling et al. 1993, Regehr et al. 2010, Cherry et al. 2013). Polar bears hunt ice-associated seals (Stirling & Archibald 1977, Bentzen et al. 2007, Thiemann et al. 2008, Sciullo et al. 2017), often from ice floes adjacent to polynyas, or by breaking through thinly covered breathing holes near frozen-over polynyas (Kiliaan & Stirling 1978, Stirling 1980, Stirling et al. 1981, Smith & Sjare 1990). Polar bear habitat selection balances optimal foraging and sea ice conditions for energy conservation and safety (Mauritzen et al. 2003a, Reimer et al. 2019), with habitat selection varying between seasons to meet energy requirements, as well as the necessity to be close to land for the breakup period in some populations (Stirling et al. 1993, McCall et al. 2016). Variation in polar bear space use and habitat selection is associated with age, reproductive status, time of year, energy expenditure, prey availability, movement capabilities, and avoidance of conspecifics (Stirling et al. 1993, Pilfold et al. 2014a, McCall et al. 2015, 2016).

While polynyas and leads might be suitable hunting habitat for polar bears, not all polynyas, nor all areas of a polynya, are equally productive (Lara et al. 1994, Ringuette et al. 2002, Karnovsky et al. 2007). Furthermore, the open water may be a barrier to polar bear movement. Bears frequently walk along the edge of wide polynyas rather than swimming across, as swimming can be metabolically costly (Stirling et al. 1993, Griffen 2018). Cubs in particular are unable to regulate body temperature in water, so mothers with offspring often avoid open

water and swimming (Blix & Lentfer 1979, Aars & Plumb 2010, Pilfold et al. 2017). Despite the persistence of polynyas and leads and their potential importance in influencing bear movement dynamics, no quantitative measurements have been made.

The largest, recurring flaw lead (hereafter lead) in Canada forms around the perimeter of Hudson Bay, most prominently along the western coast as northwesterly winds drive pack ice away from the fast ice between Churchill, Manitoba and Coral Harbour, Nunavut (Figure 1; Hare & Montgomery 1949, Stirling et al. 1977, Dunbar 1981, Markham 1986, Stewart & Barber 2010). The lead ranges from a few meters to more than 50 km wide, with a mean width of 8 km (Hare & Montgomery 1949, Danielson 1971, Stirling et al. 1977). The lead falls within the home ranges of three polar bear populations, Foxe Basin, Southern Hudson Bay, and Western Hudson Bay (IUCN/SSC Polar Bear Specialist Group 2018).

The objective of this study was to examine the use of the lead by adult female polar bears in western Hudson Bay, Canada. We examined the use of the lead: 1) as an attractant (e.g., prey availability), or 2) as a barrier to movements. We compared the use of the lead: 1) spatially within the Bay, 2) at different times of the ice-covered season, and 3) based on reproductive status. We used synthetic aperture radar (SAR) to map the lead, and explore the temporal dynamics of the maximum width and total area of the lead, and how these affect polar bear movements. We used global positioning system (GPS) satellite telemetry to evaluate movement metrics of polar bears relative to the lead by calculating 1) distance to the lead, 2) relative movement direction, 3) first passage time (FPT), 4) turning angles, and 5) crossing rate.

METHODS

Study Area and Population

Hudson Bay is an inland sea, roughly 10^6 km^2, with a mean depth of 125 m, and an ice thickness up to 1.5 m (Jones & Anderson 1994, Landy et al. 2017). Hudson Bay is ice-covered in winter and ice-free in summer, with maximum ice cover occurring in late April/early May (Stewart & Barber 2010). Freeze-up of the Bay begins in October along the northwest coastline, and breakup begins in late May along the lead in the northwest as currents and wind push ice southeast (Stirling et al. 1977, Stewart & Barber 2010). The Western Hudson Bay polar bear population shows high fidelity to the areas in the Bay adjacent to the Nunavut, Manitoba, and north-western Ontario coasts (IUCN/SSC Polar Bear Specialist Group 2018). Most Western Hudson Bay polar bears spend the ice-free season on land in Manitoba, then travel north along the shore as the Bay freezes to spend the ice-covered season on the sea ice until breakup (Stirling et al. 1977, Derocher & Stirling 1990).

Flaw Lead Mapping

We mapped the western Hudson Bay lead using SAR imagery obtained from the Canadian Space Agency's RADARSAT-2 satellite, with a resolution of 62.3 m x 121 m (Canadian Space Agency 2013). The SAR imagery differentiated between open water and ice within the Bay. Daily open water in Hudson Bay was mapped by merging daily partial SAR images of the Bay, and incomplete areas were temporally interpolated using the two previous and two subsequent days images. To map the lead, all open water adjacent to landfast ice was extracted using the 'raster', 'rgeos', 'sp', and 'rgdal' R packages, as well as geoprocessing tools in QGIS version 3.4.5 (Pebesma & Bivand 2005, Bivand et al. 2013, 2019, Bivand & Rundel 2019, Hijmans 2019b, QGIS Development Team 2019, R Core Team 2019). Landfast ice was extracted from the Canadian Ice Service Arctic Regional Sea Ice Charts in SIGRID-3 Format

(Canadian Ice Service 2009). Weekly sea ice charts were available for the whole period except January – March of 2010 – 2011, when biweekly sea ice charts were used. Landfast ice was restricted to the Western Hudson Bay population border (IUCN/SSC Polar Bear Specialist Group 2018). Because landfast ice was used to extract the open water, the lead was estimated for the period when >95% of the Hudson Bay coastline was bordered by landfast ice; approximately late December to mid-May from 2009 – 2018 (Table A1 in Appendix). Days without a complete SAR image of the Western Hudson Bay population border were removed from analysis. Ice misclassified as water was manually removed from the lead boundary using QGIS by visually comparing to images retrieved from the National Aeronautics and Space Administration (NASA) WorldView database of Moderate Resolution Imaging Spectroradiometer (MODIS) satellite imagery (National Aeronautics and Space Administration, QGIS Development Team 2019).

We calculated the maximum width of the lead per day as the largest distance from the lead border furthest from the coast, to the closest point on the landfast ice (Figure A1 in Appendix) using the 'geosphere' R package (Hijmans 2019a). The width of the lead at the point closest to the bear's location (see section "Polar Bear Telemetry") was also calculated in the same manner. The total area of the lead was calculated per day using the 'raster' R package (Hijmans 2019b). Friedman's test was performed to compare the lead maximum width and total area for each month using daily images, followed by *post hoc* Wilcoxon signed-rank tests ($\alpha = 0.05$). The lead area and width, and the width of the lead at the point closest to the bear's location were used as covariates in subsequent models.

Polar Bear Telemetry

Seventy-three adult female polar bears (≥5 years old) were captured and fitted with GPS Argos® satellite-linked collars (accuracy 30 m; Telonics Inc., Mesa, AZ; (Tomkiewicz et al. 2010), and tracked from December 2009 – May 2018 as part of ongoing, long-term research on the ecology of Western Hudson Bay polar bears (e.g., Ramsay & Stirling 1988, Derocher & Stirling 1995, Stirling et al. 1999, Regehr et al. 2007, Lunn et al. 2016). All bears were collared on land in or near Wapusk National Park, Manitoba before the bears returned to the sea ice (Figure 1). Bears were remotely immobilized using Zoletil® (Laboratories Virbac, Carros, France) for deploying the collars (Stirling et al. 1989). Adult male polar bears were not tracked because their necks are larger than their heads so they cannot wear collars. GPS collars tracked polar bear locations in 4 h intervals for up to four years. All collars had a timed-release mechanism to drop off on a predefined date, or collars were removed upon recapture. Bears were already on ice at the beginning of the study period in December, however, mothers with cub(s)-of-the-year (COY) return to ice in March (Stirling et al. 1977). We used a NAD83 (CSRS) Teranet Ontario Lambert (EPSG:5321) projection (https://epsg.io/5321) for telemetry locations. The University of Alberta BioSciences Animal Care and Use Committee (No. AUP00000033), and the Environment and Climate Change Canada's Western and Northern Animal Care Committee approved the animal capture and handling procedures, in accordance with the wildlife guidelines of the Canadian Council on Animal Care (https://www.ccac.ca/Documents/Standards/Guidelines/Wildlife.pdf).

Reproductive status (presence and age of offspring) was recorded at capture, and inferred from the time of collaring, unless confirmed if recaptured in a subsequent year. Reproductive status included 3 categories: lone female, mother with COY, and mother with yearling(s) (YRLG). Recaptured bears with a whole litter loss were removed from analysis for the previous

year (December – May). Bears with stationary movements on land from September – March were presumed to be denning (Stirling et al. 1977), and reproductive status was inferred to be mother with COY for that year, and lone for the previous spring (March – May) during polar bear breeding season (Lønø 1970, Ramsay & Stirling 1986). Cubs typically remain with mothers until 2 years of age (Ramsay & Stirling 1986, Ramsay & Stirling 1988), therefore, mothers with YRLG were presumed to be lone females by the following spring, unless otherwise confirmed with recapture data. Bears with unknown reproductive status were removed from analysis for the period the status was unknown. When not accounting for reproductive status, bears refers to all bears.

Polar bear locations were filtered using the 'argosfilter' R package (Freitas 2012) to remove biologically impossible speeds (>10 km h^{-1}; Amstrup et al. 2000, Parks et al. 2006), and locations that deviated from the path >25 km or >50 km with turning angles of >165° or >155°, respectively (Freitas et al. 2008a, 2008b). Missing locations at 4 h intervals were estimated using the 'crawl' R package (Johnson et al. 2008) to fit a continuous-time correlated random walk (CRAWL) model using the Kalman-filter. Missing locations were estimated if the time gap between original locations was >4 h but ≤24 h. To find the largest permissible time gap to be interpolated using CRAWL without significantly affecting statistical analysis, 10-70% of locations were randomly removed from 5 tracks of 2 bears with >250 locations per track. The removed locations were then interpolated using CRAWL. FPT was calculated on the original tracks and the interpolated tracks, and compared by calculating a Spearman's rank correlation coefficient ($\alpha = 0.05$) (see section "First Passage Time").

Drifting sea ice adds an involuntary component to the overall movement of polar bears (Mauritzen et al. 2003b, Auger-Méthé et al. 2016). The ice drift component was removed from

overall movement to obtain the voluntary component for use in movement-based analysis. We estimated the ice drift component using data from the National Snow and Ice Data Center (Polar Pathfinder Daily 25 km EASE-Grid Sea Ice Motion Vectors) (Tschudi 2019). Ice drift was temporally and spatially interpolated using inverse distance weighting to estimate the ice drift vector at each polar bear location (Li & Heap 2011), then subtracted from polar bear movement vectors to determine the voluntary movement of the polar bear (Auger-Méthé et al. 2016, Togunov et al. 2017, 2018).

Bear Movements

The 100% minimum convex polygon (MCP; Figure 1) of all bears was calculated using the 'adehabitatHR' R package (Calenge 2006) to map the maximum extent of Hudson Bay used by bears in the study. The median voluntary step length for all bears and years was calculated using consecutive points separated by 4 h (Figure 2a). The median voluntary daily displacement was calculated for all bears and years, using days with all 6 locations (Figure 2b). The Bay was divided into habitat categories (Figure 3), where habitat ≤1 median step length from the lead was considered to be 'on' the lead, habitat >1 step length but ≤2 times median daily displacement was considered 'near' the lead, and habitat >2 times median daily displacement was considered 'off' the lead. We used the 'on' habitat to generate 100 available locations per day bears were on the lead, and found the width of the lead closest to the available locations (see section "Flaw Lead Mapping"). We fit a generalized linear mixed effect model to predict use of the lead with width closest to the location as the predictor variable. Year was used as the random effect to account for autocorrelation. A second generalized linear mixed model was fit using bears on the

lead to predict lead width closest to the bear, using month (4 categories, February – May) and reproductive status as predictor variables.

Distance to the lead was calculated as the straight line distance from the bear location to the closest point on the lead using the 'geosphere' R package (Hijmans 2019a). To test the effect of month, lead size (width and area), and reproductive status on bear distance to the lead, we fit a set of maximum likelihood linear mixed effect models. Month and lead size, as well as lead maximum width and lead total area, were correlated so they were not used as predictor variables in the same model. Two models were fit: 1) a main model predicting distance to the lead, with month (6 categories, December – May), maximum daily lead width, total daily lead area, and reproductive status as predictor variables using data from the entire study area; and 2) a second model predicting distance to the lead in March – May, using lead width closest to the bear, maximum daily lead width, daily lead area, and reproductive status as predictor variables. The model was restricted to March – May because this was when bears were closer to the lead (see section "Results: Bear Movements"). Month provided a better fit than quadratic transformed ordered day, so it was used in candidate models. Maximum daily lead width, total daily lead area, and lead width closest to the bear were tested as both linear and quadratic variables. Bears distance to the western Hudson Bay landfast ice was calculated in the same manner as the distance to lead. The same models as distance to lead were fit predicting distance to the landfast ice to test whether the bears moved closer to the lead, or the edge of the lead became closer to the bears as it widened.

We used χ^2 tests ($\alpha = 0.05$) to compare the amount of time spent on, near, and off the lead for all bears, for only bears that were on the lead at least once during the study period, by month, and based on reproductive status. The total area on, near, and off the lead for every day

included in the tests, restricted to the bears 100% MCP, represented the available habitat in each category and was used to generate the expected ratios (Figure 3). Adjusted standardized residuals were calculated to identify the habitat category where bears spent a disproportionate amount of time.

To examine how polar bear movements were affected by the lead, we calculated relative movement direction θ, which is the direction of bear movement relative to the lead ($-180° \leq \theta \leq 180°$; Figure 2c). Relative movement direction is represented by the angle between the straight-line connecting GPS points at time *t* and *t+1*, and the shortest straight-line connecting point at time *t* to the lead (McKenzie et al. 2012). Relative movement direction was divided into 3 groups: towards ($-45° \leq \theta \leq 45°$), along ($-45° > \theta > -135°$ & $45° < \theta < 135°$), and away ($-135° \leq \theta \geq 135°$) from the lead. Relative movement direction was calculated using locations representing bears overall movement. Univariate and bivariate von Mises distributions of relative movement direction for steps on, near, and off the lead, as well as for steps by month (6 categories, December – May) were calculated using the 'circular' R package (Agostinelli & Lund 2017). Using a log likelihood ratio test, we tested the null hypothesis (uniform distribution of angles) against the univariate and bivariate von Mises distributions to determine whether movement direction was random with respect to the lead. A chi-square distribution was used to test the significance of the log likelihood ratio tests ($\alpha = 0.05$). These methods are adapted from McKenzie et al. (2012) and Potts et al. (2014).

First Passage Time

FPT is a measure of an individual's use of an area by measuring how long the individual takes to enter and exit a circle of a fixed radius (Johnson et al. 1992, Fauchald & Tveraa 2003,

2006). FPT increases with increasing radius and increasing tortuosity of the path as the individual remains in the area longer, indicating higher use (Johnson et al. 1992, Fauchald & Tveraa 2003). FPT identifies the spatial scale of area restricted search (ARS), a foraging pattern where animals slow their movements to remain within an area where prey has been located (Kareiva & Odell 1987, Fauchald & Tveraa 2003).

Following Fauchald and Tveraa (2003, 2006), we calculated FPT using tracks with a minimum of 33 locations (voluntary movement) at 4 h intervals (minimum 5.5 days/track). To find the spatial scale of ARS, equally spaced locations were interpolated along the bear's track every 2 km to reduce biases in parts of the track with a higher fix rate due to a higher search rate (Fauchald & Tveraa 2006). Spatial intervals for interpolated points were tested at 1 km, 2 km, the median step length, and 5 km and tested whether FPT significantly differed using a Spearman's rank correlation coefficient. The interpolated locations were used to calculate FPT using radii ranging from 500 m to 100 km at 500 m intervals to find the radius of peak variance in $\log_{10}$-transformed FPT for each individual, which is the spatial scale at which an animal undergoes ARS (Fauchald & Tveraa 2003, 2006). A common radius, equal to the peak mean variance in $\log_{10}$-transformed FPT for all trips and all bears, was used to calculate FPT using original GPS locations (ice drift removed) to reduce individual differences to make inter-individual comparisons. FPT was calculated using the 'adehabitatLT' R package (Calenge 2006).

To test the effect of month, distance to the lead, lead width, and reproductive status on FPT, we fitted a maximum likelihood linear mixed effect model using the 'lme4' R package (Bates et al. 2015). Distance to the lead and month were correlated, so they were not used as predictor variables in the same models. FPT was $\log_{10}$-transformed to satisfy the assumption of normality of residuals. Locations were filtered at intervals equal to the radius used to calculate

FPT for modelling (Freitas et al. 2008b), and individual bear identification was used as a random effect to account for autocorrelation. Three models were fit: 1) a main model predicting FPT, with month (6 categories, December – May), distance to the lead, and reproductive status as predictor variables using data from the entire study area; 2) a second model predicting FPT in March – May, using distance to the lead, reproductive status, and lead width closest to the bear as predictor variables; and 3) a third model predicting FPT when the bears were on the lead, using month (4 categories, February – May), distance to the lead, reproductive status, and lead width closest to the bear as predictor variables. The model was restricted to March – May because this was when bears were closer to the lead (see section "Results: Bear Movements"). Distance to the lead and lead width closest to the bear were tested as both linear and quadratic variables.

To examine how distance to the lead and month affected turning angles ($-180° \leq \theta \leq 180°$; Figure 2d), the deviation from the straight-line path connecting the two previous points was calculated using the 'trajr' R package (Kareiva & Odell 1987, Fauchald & Tveraa 2003, McLean & Skowron Volponi 2018). Turning angles were calculated using locations representing voluntary movement without CRAWL interpolated points, with 4 h between consecutive points. Locations ≤30 m apart were removed to account for GPS error in stationary bears, which can introduce bias towards large turning angles (Hurford 2009). Turning angles were divided into 3 groups: low ($-45° \leq \theta \leq 45°$), turn ($-45° > \theta > -135°$ & $45° < \theta < 135°$), and reversal turn ($-135° \leq \theta \geq 135°$). Univariate and bivariate von Mises distributions were calculated using the 'circular' R package (Agostinelli & Lund 2017). Using a log likelihood ratio test, we tested the null hypothesis (uniform distribution of angles) against the univariate and bivariate von Mises distributions of turning angles on, near, and off the lead, as well as by month (6 categories,

December – May) to examine whether turning angles were random with respect to distance to the lead or month. A χ^2 distribution was used to test the significance of the log likelihood ratio tests ($\alpha = 0.05$). These methods were adapted from McKenzie et al. (2012) and Potts et al. (2014). Because movements predominantly had low turning angles (see section "Results: First Passage Time"), the proportion of turning angles on, near, and off the lead and by month were also compared using a Pearson's χ^2 test with the Marascuilo procedure ($\alpha = 0.05$) for *post hoc* analysis (Marascuilo 1966).

Flaw Lead Crossing Rate

We calculated crossing rate of the lead as a metric to estimate whether the lead posed a barrier to movement. The portion of a bear's track that was on the lead was considered a trip, and ended either when the bear moved >1 step length away from the lead, or when SAR imagery was no longer available. Following Siers et al. (2016), each trip was treated as a Bernoulli trial and assigned a response of 1 if the bear crossed the lead, or 0 if the bear did not cross before the end of the trip. A crossing was identified by locating the section of a track overlapping the lead using the 'rgeos' R package (Bivand & Rundel 2019). Crossings were visually confirmed in QGIS using images retrieved from the NASA WorldView database of MODIS satellite imagery (National Aeronautics and Space Administration, QGIS Development Team 2019). A generalized linear mixed effects model was fit to predict crossing the lead. Month (3 categories; March – May), mean lead width at the point closest to the bear for the trip, lead width closest to the bear's first location of the trip, and lead width when either the bear begins crossing, or leaves the lead without crossing were used as predictor variables. The different widths were correlated so they were not included in the same models.

All statistical analyses were completed using R version 3.6.1 (R Core Team 2019). When possible, data were transformed using $\log_{10}$ or square root transformation and tested for normality using a Shapiro-Wilk test for use in parametric tests, otherwise nonparametric tests were used. Results are presented with mean ± SE unless stated otherwise. Linear mixed effect models and generalized linear mixed effect models were fit using the 'lme4' r package (Bates et al. 2015). Unless stated otherwise, individual bear identification was used as a random effect in models to account for non-independence of measures on the same individual. Predictor variables of models were tested for correlation using a Spearman's rank correlation coefficient. The top models were selected using corrected Akaike information criterion values (AIC_c), and if the ΔAIC_c was <2, the model with fewer covariates was selected (Burnham & Anderson 2002). Significance of predictor variables in the selected top model were assessed at $\alpha = 0.05$. See appendix for a full list of candidate models for all regression analysis (Table A3, A4, A10, & A13).

RESULTS

Flaw Lead Mapping

The lead was mapped for 540 days from December 2009 – May 2018 (43.3% of the days with >95% of the Hudson Bay coastline bordered by landfast ice; Table A1 in Appendix). These were the days when imagery for the whole western Hudson Bay coastline was available. The mean number of days between images was 2.3 ± 0.2 days (range 1 – 40). The mean maximum width of the lead was 27.0 ± 1.0 (4.5 km to 145 km), while the mean total area was 3.9×10^3 km^2 (84 km^2 – 3.1×10^4 km^2; Table A2 in Appendix). Maximum width and total area in December and January did not significantly differ (Width: Wilcoxon signed-rank $z = -0.05$, $p = 0.96$; Total

area: Wilcoxon signed-rank z =-0.88, p = 0.37), therefore these months were combined for tests comparing width and area by month due to the small sample size in December (n = 23), and to account for the time period of December being less than two weeks. Daily images from December – May, 2011, 2013-2018 were used to compare the maximum width and total area. 2010 and 2012 were excluded from analysis as there were no images for May 2010 or April 2012. The maximum width (Friedman's test $\chi^2 = 83.9$ df = 4, $p < 0.001$; Table 1; Figure A2a in Appendix), and total area (Friedman's test $\chi^2 = 67.1$ df = 4, $p < 0.001$; Table 2; Figure A2b in Appendix) of the lead varied by month. The lead was widest in May (60 ± 5 km), and narrowest in March (18 ± 0.8 km). The lead had the largest total area in May (9252 ± 1035 km^2), and the smallest total area in March (2048 ± 160 km^2). The lead was significantly larger by width and area in May than all other months, and larger in April than February and March (Tables 1 & 2).

Bear Movements

Removing biologically impossible points based on speed and angle resulted in the loss of 0.13% of locations (103/78,777). The mean time gap interpolated using CRAWL was 10.6 ± 0.1 h (5 – 24 h) to generate tracks with an equal spatial interval of 4 h. The time between consecutive locations in a track before interpolation was 4.9 ± 0.03 h. Tracks contained 14.4 ± 0.4% (0-50%) interpolated points. When 50% of the locations were removed from the CRAWL test tracks, the time between consecutive points before interpolation was 8.0 ± 0.2 h. The largest time gap interpolated was 56 h, with a mean time gap of 11.8 ± 0.3 h. FPT was not significantly different between the original track and interpolated track (Spearman's rank r = 0.82, $p < 0.001$, y-intercept = 1.7, m = 0.9; Figure A3 in Appendix).

The median step length (n = 62504) for all bears and years was 3.3 km, and the median daily displacement (n = 55716) was 14 km. Bears were considered on the lead when they were ≤3.3 km from the lead, near the lead when they were >3.3 km but ≤28 km from the lead, and off the lead when they were >28 km from the lead. Bears were on narrower sections of the lead compared to the available widths of the lead (Table 3). When on the lead, all bears were on narrower sections of the lead in May than in all other months, however, mothers with YRLG were on wider sections of the lead compared to lone females and mothers with COY (Table 3).

Month and reproductive status were strong predictors of bear distance to the lead. All bears were furthest from the lead in December, and closest in May, while mothers with COY and YRLG were closer to the lead than lone females (Table 4; Table A5 & Figure A4 in Appendix). The same trends were predicted in the top main model when predicting bears distance to landfast ice (Tables A6 & A7 in Appendix). In March – May, all bears were closer to the lead on days with an intermediate maximum width of the lead, and mothers with offspring were closer to the lead than lone females (Table 4; Table A5 in Appendix).

When assessing the amount of time all bears spent in habitats on, near, and off the lead, bears spent more time off the lead and less time on and near the lead in relation to the amount of available habitat in each category ($\chi^2 = 81$ df = 2, $p < 0.001$). When using only bears that were on the lead at least once during the study, more time was spent near and on, and less time off the lead in relation to the amount of habitat available in each category ($\chi^2 = 166$ df = 2, $p < 0.001$). Of the bears that were on the lead at least once, they spent 5.1 ± 1.5% (range 0.3 – 25.6%) of their time on the lead, while only 1.8 ± 0.04% (range 0.3 – 6.9%) of the available habitat was categorized as on the lead. When bears were on the lead, they stayed for 25.9 ± 3.8 h (range ≤4 h – 108 h) before either leaving the area, or the end of the SAR imagery. Bears spent the most time

on the lead in April (χ^2 = 87 df = 5, $p < 0.001$), and near the lead in May (χ^2 = 714 df = 5, $p < 0.001$). Compared to what was expected based on the area available in each habitat category, mothers with COY spent more time off and less time near and on the lead (χ^2 = 140 df = 2, $p < 0.001$), mothers with YRLG spent more time off and less time on the lead, and the expected proportion of time near the lead (χ^2 = 14 df = 2, $p < 0.01$), and lone females spent more time near and less time off the lead, and the expected proportion of time on the lead (χ^2 = 101 df = 2, $p < 0.001$). Comparing reproductive groups, lone females spent more time on and near, and less time off the lead than mothers with COY, and mothers with YRLG spent the expected proportion of time in each habitat category (On: χ^2 = 17 df = 2, $p < 0.001$; Near: χ^2 = 209 df = 2, $p < 0.001$; Off: χ^2 = 17 df = 2, $p < 0.001$).

In all habitat categories, bear movement direction relative to the lead followed a bivariate von Mises distribution (Figure 4a-c; Table A8 in Appendix). While on the lead, bears took steps along the lead more frequently than steps towards or away, with peaks at 101° and -69°. While near and off the lead, bears took steps towards and away from the lead more frequently than steps along the lead. When near the lead, the predominant relative movement direction was towards the lead, with a more concentrated peak at -23°. When off the lead, the relative movement direction had similar concentrations of angles around the peaks at 149° and -31°. All months had bivariate von Mises distributions of movement directions relative to the lead, with movements towards and away from the lead occurring more frequently than along the lead (Figure 4d-i; Table A8 in Appendix). Bear movements were predominantly away from the lead in December and February, and towards the lead in January, and March – May.

First Passage Time

FPT was calculated using 210 continuous 4 h interval tracks from 59 bears (81% of all points). The tracks used for FPT were 39.7 ± 3.6 days long (5.5 to 182.9 days). A radius of 2.5 km, which is equivalent to the peak of the mean variance of $\log_{10}$-transformed FPT, was used to calculate FPT (Figure A5 in Appendix). FPT had a mean of 9.3 ± 0.04 h (range 0.3 to 163.2 h; n = 49,602). Using a spatial scale of 1 km, 2km, 3.3 km, and 5 km did not significantly change the resulting FPT (Table A9 in Appendix).

When predicting FPT in December – May (main model), month and reproductive status were strong predictors of FPT. FPT was significantly longer in March than all other months except February, and mothers with YRLG had the shortest FPT (Table 5; Table A10 in Appendix). When predicting FPT in March – May, FPT increased as distance to the lead increased (Table 5; Table A10 in Appendix). When predicting FPT on the lead, FPT decreased with increasing width of the lead (Table 5; Table A10 in Appendix). When including month as a predictor for this model, January and February were pooled due to small sample size (n = 5), and all points were within 26 days.

The turning angle distributions differed from uniform in all habitat categories and in all months, following bivariate and univariate von Mises distributions (Figure 5; Table A8 in Appendix). Bear turning angles were predominantly low when on and off the lead, and predominantly turned when near the lead. Bears travelled with a higher proportion of reversal turns near the lead than on or off the lead ($\chi^2 = 50$ df = 4, $p < 0.001$). Bear turning angles were predominantly low in all months, however, bears had a higher proportion of low turning angles in December than any other month, and fewer reversal turns than February – May ($\chi^2 = 396$ df = 10, $p < 0.001$). January had a higher proportion of low turning angles and lower proportion of reversal turns compared to March – May.

Flaw Lead Crossing Rate

Crossing rate of the lead was calculated using tracks from 23 bears that were on the lead. 50% (23/46) of the tracks resulted in crossings of the lead (Figure 6; Table A12 in Appendix). Of the bears that crossed the lead, they spent 16 ± 4.4 h (range 9 to 76 h) on the lead before crossing. The trips in January (n = 2), February (n = 2), and March (n = 9) were pooled for modelling due to small sample size in these months, and the width of the flaw lead did not significantly differ in these months. Reproductive status was also not used as a predictor in the model due to small sample size. Bears were less likely to cross the lead in April and May than January – March (Table 6; Table A14 in Appendix). Bears crossed 39% (13/33) of the time in April and May, while bears crossed 80% of the time in February – March (10/13).

DISCUSSION

This study quantitatively examined use of the western Hudson Bay lead by Western Hudson Bay adult female polar bears and found that use varied temporally, spatially, and by reproductive status. Adult female polar bears used habitat further from the lead early in the winter, but closer to it as the on-ice season progressed. Studies examining space use of Western Hudson Bay polar bears reached similar conclusions in relation to the shore (Parks et al. 2006, McCall et al. 2015, 2016). Furthermore, bears were closer to the lead in April and May, when it was a more prominent feature, but spent more time near narrower sections, with mothers with COY found on the narrowest sections. Similar to Stirling et al. (1993), we also found evidence polar bears travel along wider polynyas rather than across them. Collectively, these findings suggest that while the lead is an attractant to bears later in the on-ice season, a wider lead might

deter crossing and restrict movements, particularly for mothers with COY, but likely would not be a complete barrier to movements.

Movement analysis can be negatively affected by irregular GPS fix rates, particularly by introducing bias to step length and turning angle calculations, both of which are incorporated into FPT (Fauchald & Tveraa 2003, 2006, Frair et al. 2010). GPS collars do not always provide a position for every fix, often due to interference from habitat features such as open water through the submersion of antennas on the collars of swimming bears (D'Eon et al. 2002, Hebblewhite et al. 2007, Frair et al. 2010, Pilfold et al. 2017). Nonetheless, missing GPS locations were interpolated using CRAWL, which did not significantly affect FPT, but allowed calculating movement rates using longer tracks at a uniform temporal scale.

The use of high-resolution SAR imagery allowed the detection of smaller leads to investigate the temporal and spatial variation in the size of the lead, and the effects of its size on polar bear movements that otherwise might have been missed using lower resolution data. Habitat studies (McCall et al. 2016, de la Guardia et al. 2017) have used passive microwave sensors, such as advanced microwave scanning radiometer (AMSR-E and AMSR2) and Special Sensor Microwave/Imager (SSM/I), with resolutions of 6.25 km and 25 km, respectively (Cavalieri et al. 1996, Spreen et al. 2008). SAR imagery allowed the detection of open water patches <1 km wide. In addition, SAR is a useful tool for characterizing sea ice types and open water because it can detect small changes in surface texture (McCandless Jr. 2004, Onstott & Shuchman 2004). SAR backscatter coefficient values differentiate between grey tones of the SAR images, with each tone representing a different ice type and open water (Onstott & Shuchman 2004, Freitas et al. 2012). SAR imagery also facilitates the mapping of sea ice year-round and is unrestricted by weather, cloud cover, and light (McCandless Jr. 2004, Onstott &

Shuchman 2004). The temporal gaps in the SAR imagery we used, however, might have underestimated of the number of bears on the lead, the amount of time spent on the lead, or the number of crossings of the lead. Nevertheless, our study demonstrates the utility of SAR imagery in examining movements of ice associated species relative to fine-scale environmental features.

The greater amount of time spent on and near the lead in April and May coincided with seal pupping and peak seal haul out, when seals are more abundant and accessible to bears, and when bears prepare for the ice-free season fast (McLaren 1958, Ramsay & Stirling 1988, Hammill & Smith 1991, Stirling & Øritsland 1995, Lunn et al. 1997). Western Hudson Bay polar bears primarily consume ringed seals, which are likely easier to hunt than other seals due to their widespread distribution and smaller size, followed by bearded seals and harbour seals (Stirling & McEwan 1975, Thiemann et al. 2008, Sciullo et al. 2017). Ringed seals prefer high-ice concentrations with small cracks, and are found in a higher density in stable landfast ice or in consolidated pack ice, where they can haul-out and build birth lairs (Lunn et al. 1997, Wiig et al. 1999, Chambellant 2010, Chambellant et al. 2012, Pilfold et al. 2014b). Bearded seals are most abundant near leads along the floe edge, or in moving pack ice (Stirling & Archibald 1977, Stirling et al. 1993, Lunn et al. 1997, Chambellant et al. 2012). Bearded seals are larger than ringed seals, which gives them a higher caloric value, but might make them harder for smaller bears to hunt (Stirling & Archibald 1977, Thiemann et al. 2008, Pilfold et al. 2012, Sciullo et al. 2017). Harbour seals in western Hudson Bay are concentrated in shallow coastal waters along the lead (Mansfield 1967, Bajzak et al. 2013). The greater amount of time spent closer to the FLP in spring when bears are hyperphagic and prioritizing hunting suggests bears are attracted to the prey there (McLaren 1958, Stirling & McEwan 1975, Ramsay & Stirling 1988, Chambellant et al. 2012).

Slower movements and large turning angles are characteristic of area restricted search and indicative of hunting, where an animal frequently turns to remain within an area with prey (Kareiva & Odell 1987, Fauchald & Tveraa 2003). Our results suggest the area near the FLP is important hunting habitat for polar bears, particularly for lone females during seal pupping season in May, as their movements slowed and they turned more frequently, resulting in more time spent in this area (Kovacs et al. 1996, Lunn et al. 1997, Chambellant et al. 2012, Kovacs 2018). These results align with findings from the Beaufort Sea that suggest active ice is optimal foraging habitat for polar bears in April and May (Reimer et al. 2019). These movements, however, may also be indicative of mating behaviour in lone females, as mating has been shown to restrict bears movements (Stirling et al. 2016). Conversely, faster, more directed movements along a linear feature with high prey density can also be indicative of hunting because linear features can act as a corridor that allows predators to travel quicker and increase prey encounter rate (James & Stuart-Smith 2000, McKenzie et al. 2012, Dickie et al. 2017). The lead is a linear patch with high prey density (Smith 1975, Lunn et al. 1997, Chambellant et al. 2012, Bajzak et al. 2013), suggesting that the faster movements along the lead with fewer turns is an effort to increase encounter rates. We found that bears did not spend a lot of time on the lead, which might indicate they quickly encountered prey, then moved off the lead. Bears might have left the lead before encountering prey, however, if they found it to be a more challenging environment to conserve energy (Mauritzen et al. 2003a, Cherry et al. 2013, Pilfold et al. 2014a, Reimer et al. 2019), as open water can make travel more difficult or energetically costly (Monnett & Gleason 2006, Durner et al. 2011, Griffen 2018).

While the shape and higher prey density close to the lead might increase encounter rate and make it prime habitat for hunting (Stirling 1980, Chambellant et al. 2012, Bajzak et al. 2013,

Dickie et al. 2017), between hunts, bears may select for habitat off the lead as a retreat for safety (Mauritzen et al. 2003a, Durner et al. 2009). Furthermore, using areas away from the lead may help bears conserve energy because travelling in dynamic ice conditions close to the lead can increase energy expenditure (Mauritzen et al. 2003a, Cherry et al. 2013, Pilfold et al. 2014a, Reimer et al. 2019). In contrast, travelling over more consolidated ice may decrease energy expenditure (Monnett & Gleason 2006, Durner et al. 2011). While in retreat habitat off the lead, slower movements suggest bears conserve energy between hunts, or use area restricted search to hunt when prey densities are lower (Lunn et al. 1997, Fauchald & Tveraa 2003, Mauritzen et al. 2003a).

While the FLP might attract both lone females and mothers with offspring because of the availability of prey, our results suggest mothers with COY avoid or limit the amount of time spent by the lead, and instead use areas off the lead, likely to protect cubs from the threat of infanticide by adult males (Stirling et al. 1993, Derocher & Wiig 1999, Amstrup et al. 2006, Pilfold et al. 2014a, McCall et al. 2015). Infanticide by males has been associated with nutritional stress due to melting sea ice (Taylor et al. 1985, Amstrup et al. 2006). Adult males may be attracted to areas close to the lead because of hunting opportunities, or because of the presence of lone females, but their habitat preferences are poorly understood. Adult males are the dominant class, so they will likely be found in the highest-quality habitat, such as areas more suited to hunting (Stirling et al. 1993, Pilfold et al. 2014a). Adult males feed more frequently on bearded seals than other age and sex classes (Thiemann et al. 2008, 2011, Sciullo et al. 2017, Johnson et al. 2019), therefore they are expected to be found in areas where bearded seals are abundant, such as near the floe edge (Lunn et al. 1997, Chambellant et al. 2012). Adult males are also attracted to areas with lone females for mating (Ramsay & Stirling 1986, Amstrup et al.

2006, Pilfold et al. 2014a, Sciullo et al. 2017), and lone females use areas closer to the western Hudson Bay coastline (McCall et al. 2015) near the lead. The abundance of bearded seals which adult females also frequently feed on may attract them to areas closer to the lead (Thiemann et al. 2008, 2011, Sciullo et al. 2017, Johnson et al. 2019). Therefore, since adult males are expected to be found closer to the lead due to the presence of bearded seals and lone females, mothers with COY might avoid or limit their time in this area. Mothers with COY have larger home ranges and use habitats further from shore than lone females (McCall et al. 2015), suggesting mothers with COY spend more time off the lead, but come close for short periods. Mothers with COY may limit their time on the lead, and retreat to areas further off the lead for safety, as opposed to lone females that can safely stay closer to prime hunting habitat (Mauritzen et al. 2003a, Pilfold et al. 2014a). Although our top model predicting distance to the lead suggested lone females were further from the lead, this resulted from the study period excluding lone females departure from land, but including mothers with COY departure from land in March (Stirling et al. 1977), putting them in closer proximity to the lead.

Polar bears may also move off the lead between hunts to avoid open water in the lead and reduce the chances of swimming, which has a higher energetic cost than travelling on ice due to bears being relatively inefficient swimmers (Fish 1996, Monnett & Gleason 2006, Durner et al. 2011, Griffen 2018). Polar bears might avoid spending extended periods of time near open water, and instead retreat after hunting on the lead to more consolidated pack ice where it might be easier to conserve energy (Mauritzen et al. 2003a, Derocher et al. 2004). Ice becomes less consolidated in April and May, and Hudson Bay is becoming increasingly more fragmented with more open water, which is expected to increase bears energetic costs (Sahanatien & Derocher 2012). Furthermore, swimming increases the risk of mortality, particularly in young, but also in

adult polar bears (Blix & Lentfer 1979, Monnett & Gleason 2006, Aars & Plumb 2010, Pagano et al. 2012), as small bears, including adults in poor body condition, may not produce enough body heat to overcome heat loss from long swims (Griffen 2018). Consequently, mothers with young cubs are more likely to avoid open water and swim less than lone adults (Blix & Lentfer 1979, Aars & Plumb 2010, Pilfold et al. 2017). While bears can make long distance swims, Western Hudson Bay polar bears undergo fewer long distance swims than other populations, and most occur when returning to land for the ice-free season (Pilfold et al. 2017). We found that bears were most likely to cross the lead when it was narrower, suggesting bears avoided unnecessary long swims. Similar to other species that adapt to linear features by crossing at narrower locations (Rico et al. 2007, Graham et al. 2010, Siers et al. 2016), polar bears may adapt to the lead by avoiding wider sections of the lead, or by travelling along the lead to cross at narrower locations. While the lead is not expected to prevent bears from crossing, they may be deterred from crossing a wider lead, which might restrict their movements.

From freeze-up until the end of December, bears prioritize offshore travel (Parks et al. 2006, McCall et al. 2015, 2016), which coincides with our findings of faster movements away from the lead in December, with a higher frequency of small turning angles; behaviours that are characteristic of travelling (Kareiva & Odell 1987, Fauchald & Tveraa 2003, Fritz et al. 2003, Parks et al. 2006). Polar bears move further offshore when returning to ice, potentially to increase the chance of encountering juvenile prey, which are easier to hunt (Pilfold et al. 2014a, McCall et al. 2016). Lastly, we found that bears remained further from the lead into February and displayed a higher frequency of large turns and slower speeds, indicating bears may be prioritizing hunting over travelling, and using ARS to remain close to kill sites (Kareiva & Odell 1987, Fauchald & Tveraa 2003).

Arctic sea ice is declining due to climate warming, resulting in a rapidly changing seascape (Stroeve et al. 2007, Kwok & Rothrock 2009, Comiso 2012, Laxon et al. 2013), and declining sea ice can negatively affect polar bear movements, access to prey, reproductive success, and survival (Stirling & Derocher 1993, Derocher et al. 2004). Sea ice breakup is occurring earlier in Hudson Bay, which might result in an earlier widening of the lead (Scott & Marshall 2010, Kowal et al. 2017). More open water might make the lead a more challenging environment for polar bears. Bears may need to swim longer distances more frequently, which could increase risk of hypothermia in cubs and negatively affect reproductive success (Blix & Lentfer 1979, Durner et al. 2011). More frequent swims will also increase energy expenditure due to the inefficiencies of swimming, and bears will require more food, or body condition may decline (Derocher et al. 2004, Durner et al. 2011, Pilfold et al. 2017, Griffen 2018). As polar bear body condition declines due to reduced sea ice (Regehr et al. 2007, Rode et al. 2012, Obbard et al. 2016, Sciullo et al. 2016), swimming may become even less efficient for bears (Griffen 2018). Furthermore, if infanticide becomes more frequent due to reduced sea ice, the lead may become more dangerous for mothers with offspring (Taylor et al. 1985, Stirling et al. 1993, Amstrup et al. 2006).

Although the lead may become more risky for bears, as longer ice-free periods increase the frequency of swims resulting in higher energy expenditure, and as the spring feeding period shortens, bears may increase risky behaviour (Derocher et al. 2004, Pilfold et al. 2017, Griffen 2018, Reimer et al. 2019). An increase in risky behaviour may result in bears selecting for habitat more suited to hunting, as opposed to safety, and spending more time closer to the lead (Reimer et al. 2019). Furthermore, more open water may increase the abundance of harbour seals along the lead, which may heighten the attraction of bears to the area (Derocher et al. 2004,

Iverson et al. 2006, Bajzak et al. 2013). Widening of the lead in response to future climate warming may increase polar bear travelling inefficiencies and, affect their ability to build up sufficient fat stores for the ice-free period.

Our methodology demonstrated the utility of SAR imagery to examine fine-scale habitat use of a top predator in an ice-covered environment. High resolution imagery allowed us to explore the spatial and temporal variation in polar bears use of the western Hudson bay lead in relation to narrow widths of the lead. Our findings showed bears used narrower sections of the lead more frequently later in the on-ice season, and lone females used the lead more frequently than mothers with COY. The lead did not prevent crossing, but there was evidence a wider lead might deter crossing. These findings suggest bears use of habitat within the Bay may be affected by a wider lead.

TABLES

Table 1. Comparison of the maximum width of the western Hudson Bay flaw lead by month. Data were based on synthetic aperture radar images from December – May, 2011, 2013 – 2018. 2010 and 2012 were excluded from analysis as there were no images for May 2010 or April 2012. Width was compared using a Wilcoxon signed-rank test. There was no significant difference in the maximum width in December and January (Wilcoxon signed-rank z = -0.05, p = 0.96), so these values were combined due to small sample size (n = 23), and to account for the time period of December being less than two weeks. Presented values are the median total area (km^2).

	Median Maximum Width (km)	February		March		April		May	
		p value	r	*p* value	r	*p* value	r	*p* value	r
Dec/Jan	20	0.07	0.17	0.03	0.20	0.20	0.12	<0.001	0.56
Feb	15	-		0.94	0.01	<0.001	0.38	<0.001	0.59
Mar	16			-		<0.001	0.33	<0.001	0.57
Apr	24					-		<0.001	0.54
May	53							-	

Table 2. Comparison of the total area of the western Hudson Bay flaw lead. Data were based on synthetic aperture radar images from December – May, 2011, 2013-2018. 2010 and 2012 were excluded from analysis as there were no images for May 2010 or April 2012. Area was compared using a Wilcoxon signed-rank test ($\alpha = 0.05$). There was no significant difference in the total area in December and January (Wilcoxon signed-rank $z = -0.88$, $p = 0.37$), so these values were combined due to small sample size ($n = 23$), and to account for the time period of December being less than two weeks. Presented values are the median total area (km^2).

	Median Total Polynya Area (km^2)	February		March		April		May	
		p value	r	*p* value	r	*p* value	r	*p* value	r
Dec/Jan	2821	0.03	0.20	<0.001	0.38	0.67	0.04	<0.001	0.38
Feb	1484	-		0.09	0.16	<0.001	0.33	<0.001	0.54
Mar	1471			-		<0.001	0.43	<0.001	0.55
Apr	2902					-		<0.001	0.42
May	6469							-	

Table 3. Covariate coefficient estimates for the top models predicting adult female polar bear use of the flaw lead, and width of the flaw lead closest to the bear when bears were on the flaw lead using generalized linear mixed models. Adult female polar bears are from the Western Hudson Bay polar bear population from December 2009 – May 2018 ($\alpha = 0.05$). Width is the width of the flaw lead at the point closest to the bear. Lone represents a lone female, and COY represents a mother with cub(s)-of-the-year.

				95% CI		
Model	Parameter	Estimate	SE	Lower	Upper	*p* value
Use	Width	-0.02	0.005	-0.03	-0.01	<0.001
	Constant	-3.01	0.08	-3.16	-2.86	<0.001
Width Closest to Bear	February	0.6	0.2	0.2	1.1	<0.01
	March	0.6	0.3	0.0	1.3	>0.05
	April	1.1	0.2	0.7	1.5	<0.001
	Lone	-1.3	0.2	-1.7	-0.9	<0.001
	COY	-1.0	0.4	-1.9	-0.2	<0.05
	Constant	8.5	0.4	7.7	9.3	<0.001

Table 4. Covariate coefficient estimates for the top models predicting adult female polar bear distance to the flaw lead using a maximum likelihood linear mixed effects model. Adult female polar bears are from the Western Hudson Bay polar bear population from December 2009 – May 2018 for the main model, and March 2010 – May 2018 for the March to May model ($\alpha = 0.05$). YRLG represents a mother with yearling(s), and COY represents a mother with cub(s)-of-the-year. Daily max width is the maximum width of the flaw lead on the date of the polar bear location.

				95% CI		
Model	Parameter	Estimate	SE	Lower	Upper	*p* value
Main Model	December	148.7	4.0	140.9	156.4	<0.001
	January	76.8	2.6	71.6	81.9	<0.001
	February	47.2	2.6	42.1	52.3	<0.001
	March	37.6	1.6	34.3	40.8	<0.001
	April	40.0	1.6	36.9	43.1	<0.001
	YRLG	-24.0	1.7	-27.4	-20.6	<0.001
	COY	-20.7	1.7	-24.0	-17.4	<0.001
	Constant	159.0	11.0	137.5	180.6	<0.001
March to	Daily Max Width	-0.0007	3.6E-05	-0.0007	-0.0006	<0.001
May	Daily Max Width^2	0.0001	9.6E-06	0.0001	0.0001	<0.001
	YRLG	-16.2	1.8	-19.9	-12.6	<0.001
	COY	-23.1	1.8	-26.6	-19.7	<0.001
	Constant	181.5	10.7	160.6	202.4	<0.001

Table 5. Covariate coefficient estimates for the top maximum likelihood linear mixed effects models predicting adult female polar bear log first passage time. Adult female polar bears are from the Western Hudson Bay polar bear population from December 2009 – May 2018 for the main model, March 2010 – May 2018 for the March to May model, and January 2010 – May 2018 for the on flaw lead model ($\alpha = 0.05$). January and February were pooled when predicting first passage time on the flaw lead due to small sample size (n = 5), and all points were within 26 days. Lone represents a lone adult female polar bears, and YRLG represents a mother with yearling(s). Distance to lead is the distance of the polar bear to the flaw lead. The lead width is the width of the flaw lead at the closest point to the polar bear.

				95% CI		
Model	Parameter	Estimate	SE	Lower	Upper	*p* value
Main Model	December	-0.20	0.05	-0.30	-0.09	<0.001
	January	-0.17	0.03	-0.23	-0.11	<0.001
	February	-0.08	0.03	-0.14	-0.02	<0.05
	April	-0.10	0.02	-0.13	-0.07	<0.001
	May	-0.15	0.02	-0.19	-0.11	<0.001
	Lone	0.11	0.02	0.07	0.15	<0.001
	COY	0.23	0.03	0.17	0.30	<0.001
	Constant	1.66	0.03	1.60	1.72	<0.001
March to May	Distance to Lead	8.2E-07	1.1E-07	6.0E-07	1.0E-06	<0.001
	Constant	1.68	0.03	1.62	1.75	<0.001
On the Flaw Lead	Lead Width	-4.6E-06	1.1E-06	-6.8E-06	-2.4E-06	<0.001
	Constant	1.83	0.12	1.58	2.07	<0.001

Table 6. Covariate coefficient estimates for the top generalized linear mixed effects model predicting adult female polar bear crossing rate of the western Hudson Bay flaw lead. Adult female polar bears are from the Western Hudson Bay polar bear population from January 2010 – May 2018 (α.= 0.05). January (n = 2), February (n = 2), and March (n = 9) were pooled because of small sample size, and the width of the flaw lead did not significantly differ in these months.

				95% CI		
Model	Parameter	Estimate	SE	Lower	Upper	*p* value
Crossing Rate	April (n =1 6)	-18.0	6.9	-31.6	-4.4	<0.01
	May (n = 17)	-15.4	6.6	-28.3	-2.5	<0.05
	Constant	8.7	0.9	7.0	10.5	<0.05

FIGURES

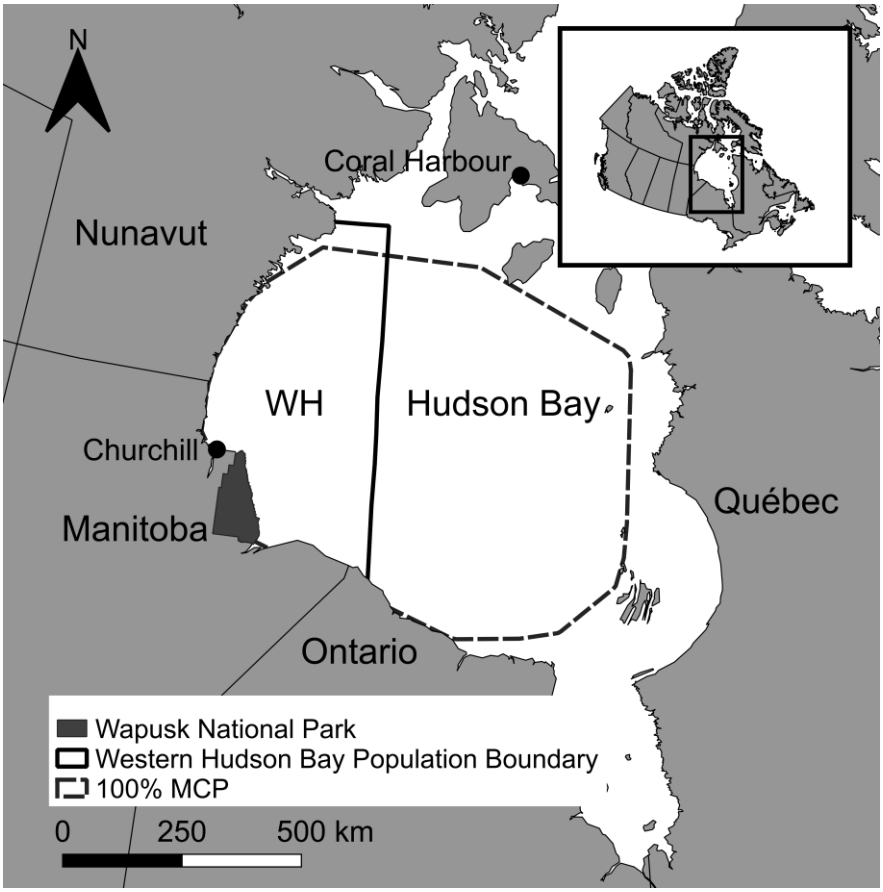

Figure 1: Map of Hudson Bay showing the Western Hudson Bay (WH) population boundary (solid line). The dashed line represents the on-ice 100% minimum convex polygon for Western Hudson Bay polar bears from December 2009 – May 2018. Wapusk National Park (dark grey shaded area) was the primary location of polar bear collar deployments.

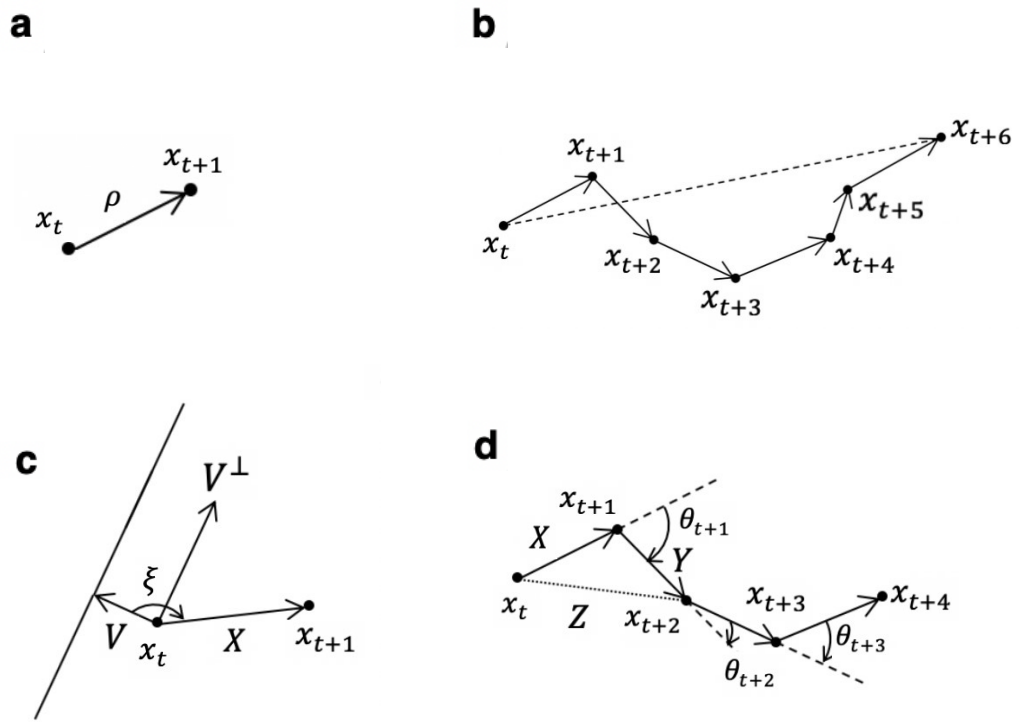

Figure 2: Movement variables used to quantify Western Hudson Bay adult female polar bears response to the western Hudson Bay flaw lead. a) Step length is the straight line distance connecting two consecutive points $\rho = \sqrt{(x_t - x_{t+1})^2 + (y_t - y_{t+1})^2}$. b) Daily displacement is the straight line connecting the first and last points in a 24 h period $\rho = \sqrt{(x_t - x_{t+6})^2 + (y_t - y_{t+6})^2}$. c) Relative movement direction is represented by the angle between the straight-line connecting two consecutive points, and the shortest straight-line to the flaw lead $\xi = sgn(X \cdot V^{\perp}) cos^{-1}\left(\frac{X \cdot V}{\|X\|\|V\|}\right)$. a) and c) follow McKenzie et al. (2012). d) Turning angle is the deviation from the straight line path connecting the two previous points $\theta_{t+1} = 180 - arccos\left(\frac{X^2+Y^2-Z^2}{2XY}\right)$, following (McLean & Skowron Volponi 2018).

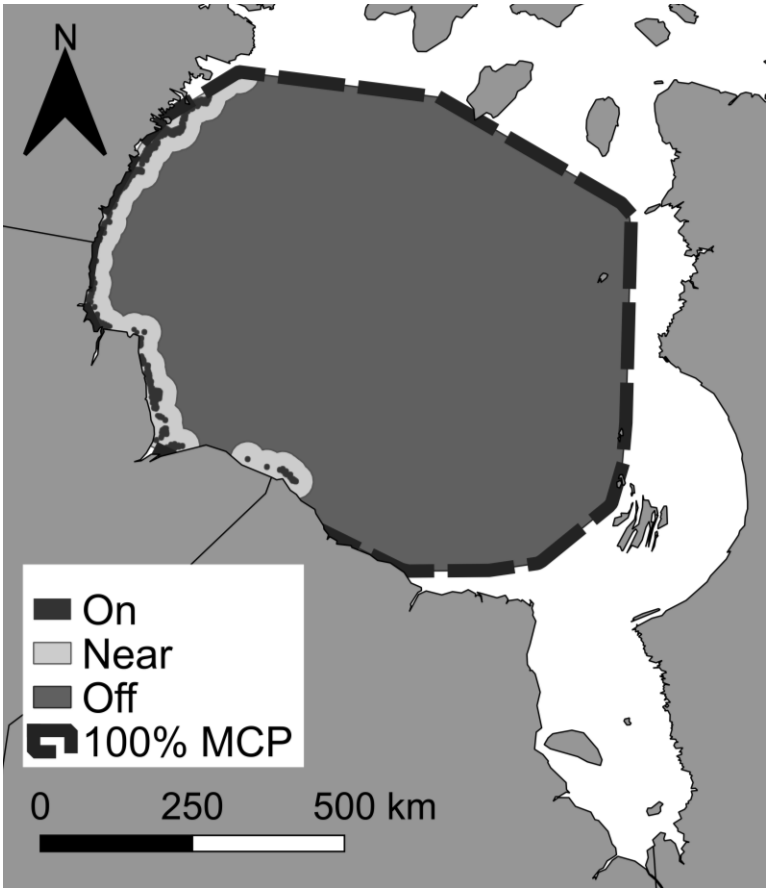

Figure 3: Map of Hudson Bay showing the habitat categories, on, near, and off the lead on February 18, 2013. Habitat ≤1 median step length from the lead was considered to be 'on' the lead, habitat >1 step length but ≤2 times median daily displacement was considered 'near' the lead, and habitat >2 times median daily displacement was considered 'off' the lead.

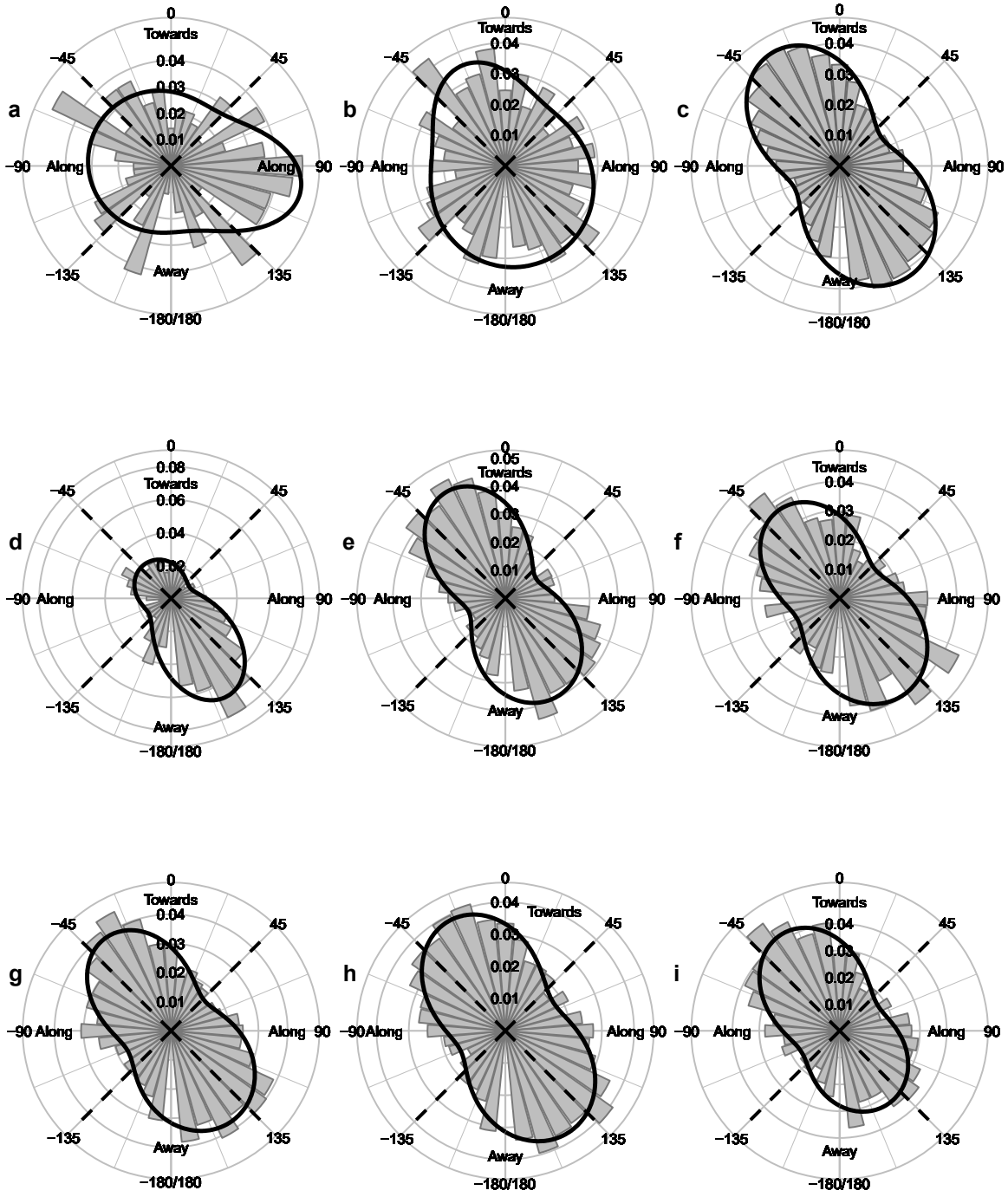

Figure 4. Direction of movements of adult female polar bears relative to the western Hudson Bay flaw lead from December 2009 – May 2018. Adult female polar bears are from the Western Hudson Bay polar bear population. Relative movement directions were divided into 3 groups:

towards ($-45° \leq \theta \leq 45°$), along ($-45° > \theta > -135°$ & $45° < \theta < 135°$), and away ($-135° \leq \theta \geq 135°$) from the flaw lead. Distributions of relative movement directions were fit a) on the flaw lead, b) near the flaw lead, c) off the flaw lead, and by month d) December, e) January, f) February, g) March, h) April, and i) May. Light grey bars represent the proportion of polar bear relative movement directions, and the solid black line represents the bivariate von Mises distribution with the best fit.

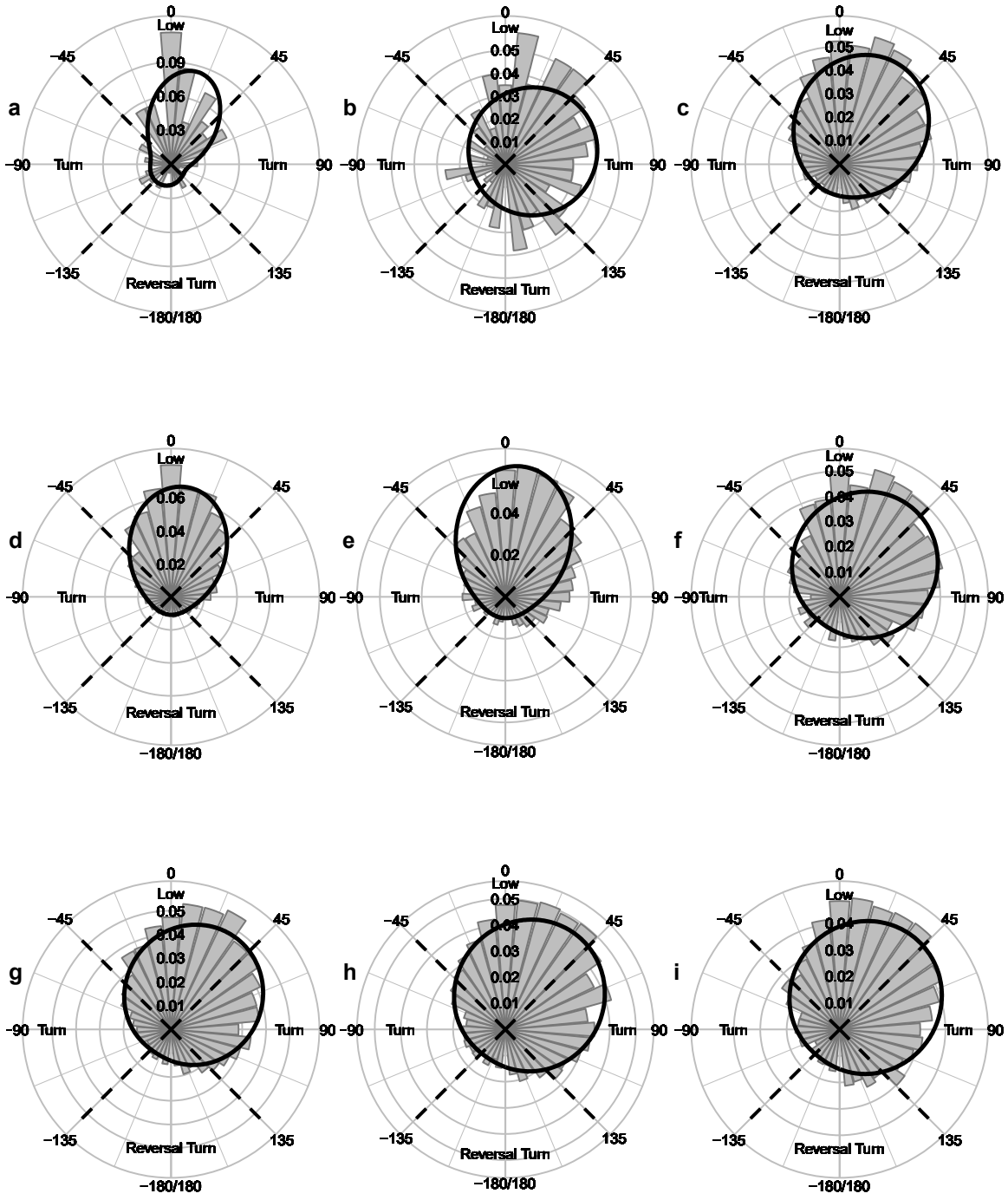

Figure 5. Turning angles of adult female polar bears in relation to the western Hudson Bay flaw lead from December 2009 – May 2018. Adult female polar bears are from the Western Hudson Bay polar bear population. Turning angles were divided into 3 groups: low ($-45° \leq \theta \leq 45°$), turn

(–45° > θ > –135° & 45° < θ < 135°), and reversal turn (–135° ≤ θ ≥ 135°). Distributions of turning angle were fit a) on the flaw lead, b) near the flaw lead, c) off the flaw lead, and by month d) December, e) January, f) February, g) March, h) April, and i) May. Light grey bars represent the proportion of the polar bear turning angles, and the solid black line represents the bivariate (a, b, d, e) and univariate (c, f - i) von Mises distributions with the best fit.

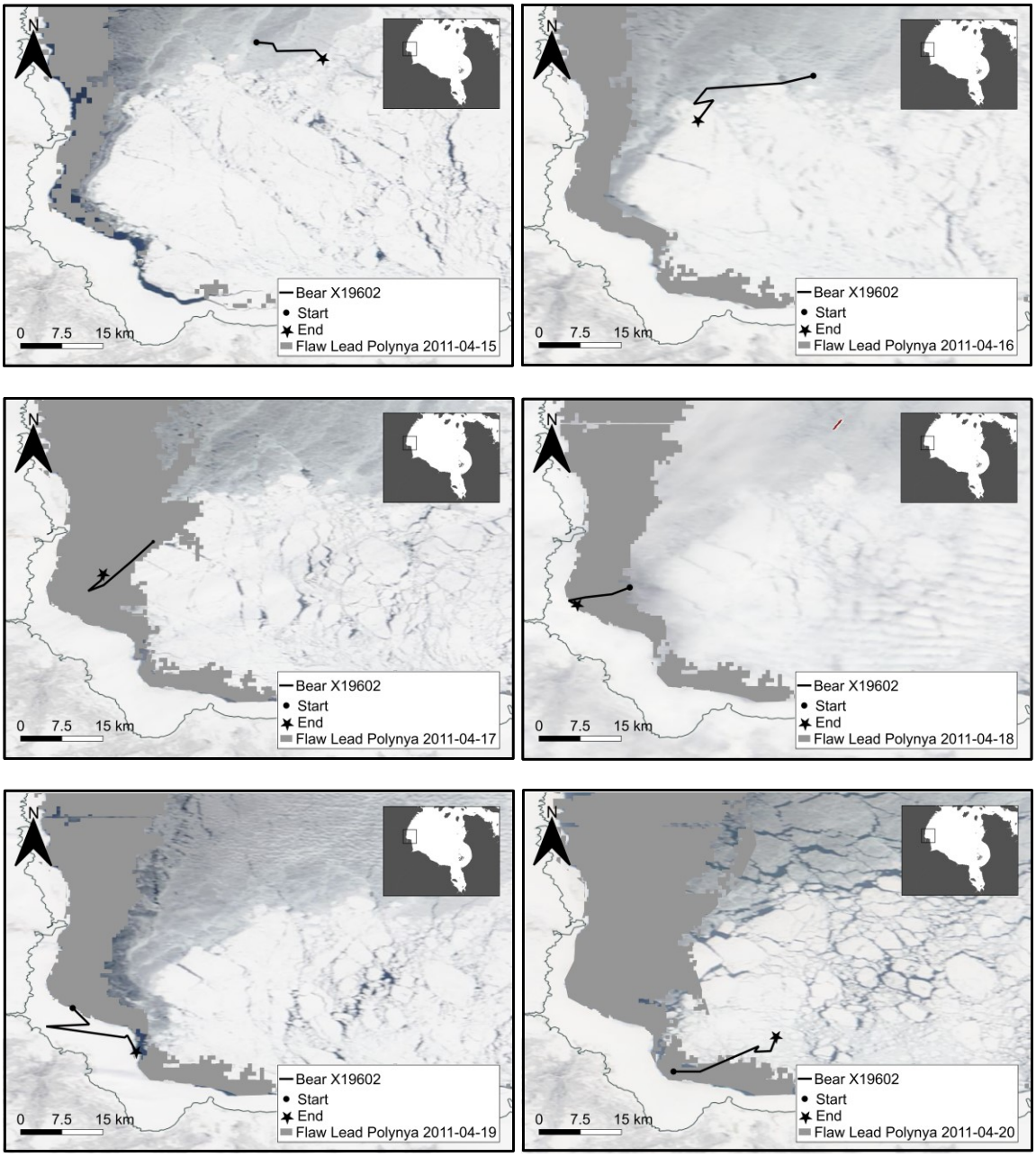

Figure 6: Track of bear X19602 (lone female) as it moves in the vicinity of the western Hudson Bay flaw lead from April 15 – 20, 2011. Bear is from the Western Hudson Bay polar bear population. Base images were obtained from the National Aeronautics and Space Administration (NASA) WorldView database of Moderate Resolution Imaging Spectroradiometer (MODIS) satellite imagery (National Aeronautics and Space Administration, QGIS Development Team 2019).

REFERENCES

Aars J, Plumb A (2010) Polar bear cubs may reduce chilling from icy water by sitting on mother's back. Polar Biol 33:557-559

Agostinelli C, Lund U (2017) R package 'circular': Circular statistics (version 0.4-93)

Amstrup SC, Durner GM, Stirling I, Lunn NJ, Messier F (2000) Movements and distribution of polar bears in the beaufort sea. Can J Zool 78:948-966

Amstrup SC, Stirling I, Smith TS, Perham C, Thiemann GW (2006) Recent observations of intraspecific predation and cannibalism among polar bears in the southern beaufort sea. Polar Biol 29:997-1002

Arrigo KR, van Dijken GL (2004) Annual cycles of sea ice and phytoplankton in cape bathurst polynya, southeastern beaufort sea, canadian arctic. Geophys Res Lett 31

Arrigo KR (2007) Chapter 7 physical control of primary productivity in arctic and antarctic polynyas. In: Smith WO, Barber DG (eds) Polynyas: Windows to the world, Vol 74. Elsevier, p 223-238

Auger-Méthé M, Lewis MA, Derocher AE (2016) Home ranges in moving habitats: Polar bears and sea ice. Ecography 39:26-35

Bajzak CE, Bernhardt W, Mosnier A, Hammill MO, Stirling I (2013) Habitat use by harbour seals (*phoca vitulina*) in a seasonally ice-covered region, the western hudson bay. Polar Biol 36:477-491

Barber DG, Massom RA (2007) Chapter 1 the role of sea ice in arctic and antarctic polynyas. In: Smith WO, Barber DG (eds) Polynyas: Windows to the world, Vol Volume 74. Elsevier, p 1-54

Bates D, Mächler M, Bolker B, Walker S (2015) Fitting linear mixed-effects models using lme4. 2015 67:48

Bentzen TW, Follmann EH, Amstrup SC, York GS, Wooller MJ, O'Hara TM (2007) Variation in winter diet of southern beaufort sea polar bears inferred from stable isotope analysis. Can J Zool 85:596-608

Bivand R, Keitt T, Rowlingson B (2019) Rgdal: Bindings for the 'geospatial' data abstraction library R package version 14-8

Bivand R, Rundel C (2019) Rgeos: Interface to geometry engine - open source ('geos') R package version 05-2

Bivand RS, Pebesma EJ, Virgilio G-R (2013) Applied spatial data analysis with r, second edition, Vol. Springer, NY

Black AL, Gilchrist HG, Allard KA, Mallory ML (2012) Incidental observations of birds in the vicinity of hell gate polynya, nunavut: Species, timing, and diversity. Arctic:145-154

Blix AS, Lentfer JW (1979) Modes of thermal protection in polar bear cubs - at birth and on emergence from the den. Am J Physiol 236:R67-74

Brown R, Nettleship DN (1981) The biological significance of polynyas to arctic colonial seabirds. Polynyas in the Canadian Arctic Canadian Wildlife Service Occasional Paper 45:59-65

Brown TA, Belt ST, Ferguson SH, Yurkowski DJ, Davison NJ, Barnett JEF, Jepson PD (2013) Identification of the sea ice diatom biomarker ip25 and related lipids in marine mammals: A potential method for investigating regional variations in dietary sources within higher trophic level marine systems. J Exp Mar Biol Ecol 441:99-104

Brown TA, Galicia MP, Thiemann GW, Belt ST, Yurkowski DJ, Dyck MG (2018) High contributions of sea ice derived carbon in polar bear (*ursus maritimus*) tissue. PLoS ONE 13:e0191631

Burnham KP, Anderson DR (2002) Model selection and multimodel inference: A practical information-theoretic approach, Vol. Springer New York

Bursa A (1963) Phytoplankton in coastal waters of the arctic ocean at point barrow, alaska. Arctic 16:239-262

Calenge C (2006) The package "adehabitat" for the r software: A tool for the analysis of space and habitat use by animals. Ecol Modell 197:516-519

Canadian Ice Service (2009) Canadian ice service arctic regional sea ice charts in sigrid-3 format, version 1. 2009-2018. Boulder, Colorado USA. : https://doi.org/10.7265/N51V5BW9.

Canadian Space Agency (2013) Earth observation satellites. Canadian Space Agency

Cavalieri DJ, Parkinson CL, Gloersen P, Zwally HJ (1996) Sea ice concentrations from nimbus-7 smmr and dmsp ssm/i-ssmis passive microwave data, version 1. Boulder, Colorado USA: https://doi.org/10.5067/8GQ8LZQVL0VL.

Chambellant M (2010) Hudson bay ringed seal: Ecology in a warming climate. In: Ferguson SH, Loseto LL, Mallory ML (eds) A little less arctic. Springer, Dordrecht, p 137-158

Chambellant M, Lunn NJ, Ferguson SH (2012) Temporal variation in distribution and density of ice-obligated seals in western hudson bay, canada. Polar Biol 35:1105-1117

Cherry SG, Derocher AE, Thiemann GW, Lunn NJ (2013) Migration phenology and seasonal fidelity of an arctic marine predator in relation to sea ice dynamics. J Anim Ecol 82:912-921

Comiso J (2010) Polar oceans from space, Vol 41. Springer Science & Business Media

Comiso JC (2012) Large decadal decline of the arctic multiyear ice cover. J Clim 25:1176-1193

D'Eon RG, Serrouya R, Smith G, Kochanny CO (2002) Gps radiotelemetry error and bias in mountainous terrain. Wildl Soc Bull:430-439

Danielson EW (1971) Hudson bay ice conditions. Arctic 24:90-+

David C, Lange B, Krumpen T, Schaafsma F, van Franeker JA, Flores H (2016) Under-ice distribution of polar cod boreogadus saida in the central arctic ocean and their association with sea-ice habitat properties. Polar Biol 39:981-994

de la Guardia LC, Myers P, Derocher A, Lunn N, van Scheltinga AT (2017) Sea ice cycle in western hudson bay, canada, from a polar bear perspective. Mar Ecol Prog Ser 564:225-233

Derocher AE, Stirling I (1990) Distribution of polar bears (*ursus maritimus*) during the ice-free period in western hudson bay. Can J Zool 68:1395-1403

Derocher AE, Stirling I (1995) Estimation of polar bear population-size and survival in western hudson-bay. J Wildlife Manage 59:215-221

Derocher AE, Wiig O (1999) Infanticide and cannibalism of juvenile polar bears (*ursus maritimus*) in svalbard. Arctic 52:307-310

Derocher AE, Lunn NJ, Stirling I (2004) Polar bears in a warming climate. Integr Comp Biol 44:163-176

Dickie M, Serrouya R, McNay RS, Boutin S (2017) Faster and farther: Wolf movement on linear features and implications for hunting behaviour. J Appl Ecol 54:253-263

Dunbar MJ (1981) Physical causes and biological significance of polynyas and other open water in sea ice. Polynyas in the Canadian Arctic Canadian Wildlife Service Occasional Paper 45:29-43

Durner GM, Douglas DC, Nielson RM, Amstrup SC and others (2009) Predicting 21st-century polar bear habitat distribution from global climate models. Ecol Monogr 79:25-58

Durner GM, Whiteman JP, Harlow HJ, Amstrup SC, Regehr EV, Ben-David M (2011) Consequences of long-distance swimming and travel over deep-water pack ice for a female polar bear during a year of extreme sea ice retreat. Polar Biol 34:975-984

Falk K, Hjort C, Andreasen C, Christensen KD and others (1997) Seabirds utilizing the northeast water polynya. J Mar Syst 10:47-65

Fauchald P, Tveraa T (2003) Using first-passage time in the analysis of area-restricted search and habitat selection. Ecology 84:282-288

Fauchald P, Tveraa T (2006) Hierarchical patch dynamics and animal movement pattern. Oecologia 149:383-395

Fish FE (1996) Transitions from drag-based to lift-based propulsion in mammalian swimming. Am Zool 36:628-641

Frair JL, Fieberg J, Hebblewhite M, Cagnacci F, DeCesare NJ, Pedrotti L (2010) Resolving issues of imprecise and habitat-biased locations in ecological analyses using gps telemetry data. Philos Trans R Soc Lond B Biol Sci 365:2187-2200

Freitas C, Kovacs KM, Ims RA, Fedak MA, Lydersen C (2008a) Ringed seal post-moulting movement tactics and habitat selection. Oecologia 155:193-204

Freitas C, Kovacs KM, Lydersen C, Ims RA (2008b) A novel method for quantifying habitat selection and predicting habitat use. J Appl Ecol 45:1213-1220

Freitas C (2012) Argosfilter: Argos locations filter R package version 063

Freitas C, Kovacs KM, Andersen M, Aars J and others (2012) Importance of fast ice and glacier fronts for female polar bears and their cubs during spring in svalbard, norway. Mar Ecol Prog Ser 447:289-304

Fritz H, Said S, Weimerskirch H (2003) Scale-dependent hierarchical adjustments of movement patterns in a long-range foraging seabird. Proc Biol Sci 270:1143-1148

Gilchrist HG, Robertson GJ (2000) Observations of marine birds and mammals wintering at polynyas and ice edges in the belcher islands, nunavut, canada. Arctic 53:61-68

Graham K, Boulanger J, Duval J, Stenhouse G (2010) Spatial and temporal use of roads by grizzly bears in west-central alberta. Ursus 21:43-56

Griffen BD (2018) Modeling the metabolic costs of swimming in polar bears (*ursus maritimus*). Polar Biol 41:491-503

Hammill MO, Smith TG (1991) The role of predation in the ecology of the ringed seal in barrow strait, northwest territories, canada. Mar Mamm Sci 7:123-135

Hammill MO (2018) Ringed seal: *Pusa hispida*. In: Würsig B, Thewissen JGM, Kovacs KM (eds) Encyclopedia of marine mammals (third edition). Academic Press, p 822-824

Hannah CG, Dupont F, Dunphy M (2009) Polynyas and tidal currents in the canadian arctic archipelago. Arctic 62:83-95

Hare FK, Montgomery MR (1949) Ice, open water, and winter climate in the eastern arctic of north america: Part ii. Arctic 2:149-164

Hebblewhite M, Percy M, Merrill E (2007) Are all gps collars created equal? A comparison of three brands for habitat-induced fix-rate bias. J Wildl Manag 71:2026-2033

Heide-Jørgensen MP, Burt LM, Hansen RG, Nielsen NH, Rasmussen M, Fossette S, Stern H (2013) The significance of the north water polynya to arctic top predators. Ambio 42:596-610

Heide-Jørgensen MP, Sinding M-HS, Nielsen NH, Rosing-Asvid A, Hansen RG (2016) Large numbers of marine mammals winter in the north water polynya. Polar Biol 39:1605-1614

Hijmans RJ (2019a) Geosphere: Spherical trigonometry R package version 15-10

Hijmans RJ (2019b) Raster: Geographic data analysis and modeling R package version 30-7

Hirche H-J, Baumann M, Kattner G, Gradinger R (1991) Plankton distribution and the impact of copepod grazing on primary production in fram strait, greenland sea. J Mar Syst 2:477-494

Horner R, Ackley SF, Dieckmann GS, Gulliksen B and others (1992) Ecology of sea ice biota. Polar Biol 12:417-427

Hurford A (2009) Gps measurement error gives rise to spurious 180 turning angles and strong directional biases in animal movement data. PLoS ONE 4

IUCN/SSC Polar Bear Specialist Group (2018) Polar bears: Proceedings of the 18th working meeting of the iucn/ssc polar bear specialist group, Vol. IUCN, Gland, Switzerland and Cambridge, UK

Iverson SJ, Stirling I, Lang SLC (2006) Spatial and temporal variation in the diets of polar bears across the canadian arctic: Indicators of changes in prey populations and environment. In: Camphuysen CJ, Boyd IL, Wanless S (eds) Top predators in marine ecosystems: Their role in monitoring and management. Cambridge University Press, Cambridge, p 98-117

James ARC, Stuart-Smith AK (2000) Distribution of caribou and wolves in relation to linear corridors. J Wildlife Manage 64:154-159

Johnson AC, Hobson KA, Lunn NJ, McGeachy D, Richardson ES, Derocher AE (2019) Temporal and intra-population patterns in polar bear foraging ecology in western hudson bay. Mar Ecol Prog Ser 619:187-199

Johnson AR, Wiens JA, Milne BT, Crist TO (1992) Animal movements and population dynamics in heterogeneous landscapes. Landscape Ecol 7:63-75

Johnson DS, London JM, Lea MA, Durban JW (2008) Continuous-time correlated random walk model for animal telemetry data. Ecology 89:1208-1215

Jones EP, Anderson LG (1994) Northern hudson-bay and foxe basin - water masses, circulation and productivity. Atmos-Ocean 32:361-374

Kareiva P, Odell G (1987) Swarms of predators exhibit "preytaxis" if individual predators use area-restricted search. Am Nat 130:233-270

Karnovsky N, Ainley DG, Lee P (2007) Chapter 12 the impact and importance of production in polynyas to top-trophic predators: Three case histories. In: Smith WO, Barber DG (eds) Polynyas: Windows to the world, Vol 74. Elsevier, p 391-410

Karnovsky NJ, Hobson KA, Iverson S, Hunt Jr GL (2008) Seasonal changes in diets of seabirds in the north water polynya: A multiple-indicator approach. Mar Ecol Prog Ser 357:291-299

Kiliaan H, Stirling I (1978) Observations on overwintering walruses in the eastern canadian high arctic. J Mammal 59:197-200

Kovacs KM, Lydersen C, Gjertz I (1996) Birth-site characteristics and prenatal molting in bearded seals (*erignathus barbatus*). J Mammal 77:1085-1091

Kovacs KM (2018) Bearded seal: *Erignathus barbatus*. In: Würsig B, Thewissen JGM, Kovacs KM (eds) Encyclopedia of marine mammals (third edition). Academic Press, p 83-86

Kowal S, Gough WA, Butler K (2017) Temporal evolution of hudson bay sea ice (1971–2011). Theor Appl Climatol 127:753-760

Kwok R, Rothrock D (2009) Decline in arctic sea ice thickness from submarine and icesat records: 1958–2008. Geophys Res Lett 36

Landy JC, Ehn JK, Babb DG, Thériault N, Barber DG (2017) Sea ice thickness in the eastern canadian arctic: Hudson bay complex & baffin bay. Remote Sens Environ 200:281-294

Lara RJ, Kattner G, Tillmann U, Hirche H-J (1994) The north east water polynya (greenland sea). Polar Biol 14:483-490

Laxon S, Peacock N, Smith D (2003) High interannual variability of sea ice thickness in the arctic region. Nature 425:947

Laxon SW, Giles KA, Ridout AL, Wingham DJ and others (2013) Cryosat-2 estimates of arctic sea ice thickness and volume. Geophys Res Lett 40:732-737

Lentfer JW (1972) Polar bear: Sea ice relationships. Bears: Their Biology and Management 2:165-171

Li J, Heap AD (2011) A review of comparative studies of spatial interpolation methods in environmental sciences: Performance and impact factors. Ecol Inform 6:228-241

Lønø O (1970) The polar bear (*ursus maritimus* phipps) in the svalbard area. Norsk Polarinstitutt Skrifter 149:1–115

Lunn N, Stirling I, Nowicki S (1997) Distribution and abundance of ringed (*phoca hispida*) and bearded seals (*erignathus barbatus*) in western hudson bay. Can J Fish Aquat Sci 54:914-921

Lunn NJ, Servanty S, Regehr EV, Converse SJ, Richardson E, Stirling I (2016) Demography of an apex predator at the edge of its range: Impacts of changing sea ice on polar bears in hudson bay. Ecol Appl 26:1302-1320

Mansfield AW (1967) Distribution of the harbor seal, *phoca vitulina* linnaeus, in canadian arctic waters. J Mammal 48:249-257

Marascuilo LA (1966) Large-sample multiple comparisons. Psychol Bull 65:280-290

Markham W (1986) The ice cover. In: Elsevier oceanography series, Vol 44. Elsevier, p 101-116

Martin S (2001) Polynyas. In: Steele JH (ed) Encyclopedia of ocean sciences (second edition). Academic Press, Oxford, p 540-545

Mauritzen M, Belikov SE, Boltunov AN, Derocher AE and others (2003a) Functional responses in polar bear habitat selection. Oikos 100:112-124

Mauritzen M, Derocher AE, Pavlova O, Wiig O (2003b) Female polar bears, *ursus maritimus*, on the barents sea drift ice: Walking the treadmill. Anim Behav 66:107-113

McCall AG, Derocher AE, Lunn NJ (2015) Home range distribution of polar bears in western hudson bay. Polar Biol 38:343-355

McCall AG, Pilfold NW, Derocher AE, Lunn NJ (2016) Seasonal habitat selection by adult female polar bears in western hudson bay. Popul Ecol 58:407-419

McCandless Jr. SW, & Jackson, C. R. (2004) Chapter 1: Principles of synthetic aperture radar. In: Jackson CR, & Apel, J.R. (ed) Synthetic aperture radar marine user's manual. US Department of Commerce, Washington, DC, p 1-24

McKenzie HW, Merrill EH, Spiteri RJ, Lewis MA (2012) How linear features alter predator movement and the functional response. Interface Focus 2:205-216

McLaren IA (1958) The biology of the ringed seal (*phoca hispida* schreber) in the eastern canadian arctic, Vol. Fisheries Research Board of Canada Ottawa

McLean DJ, Skowron Volponi MA (2018) Trajr: An r package for characterisation of animal trajectories. Ethology 124:440-448

Mei Z-P, Legendre L, Gratton Y, Tremblay J-É, LeBlanc B, Klein B, Gosselin M (2003) Phytoplankton production in the north water polynya: Size-fractions and carbon fluxes, april to july 1998. Mar Ecol Prog Ser 256:13-27

Monnett C, Gleason JS (2006) Observations of mortality associated with extended open-water swimming by polar bears in the alaskan beaufort sea. Polar Biol 29:681-687

National Aeronautics and Space Administration Worldview

Obbard ME, Cattet MR, Howe EJ, Middel KR and others (2016) Trends in body condition in polar bears (*ursus maritimus*) from the southern hudson bay subpopulation in relation to changes in sea ice. Arctic Science 2:15-32

Onstott R, Shuchman R (2004) Chapter 3: Sar measurements of sea ice. In: Jackson CR, & Apel, J.R. (ed) Synthetic aperture radar marine user's manual. US Department of Commerce, Washington, DC, p 81-115

Pagano AM, Durner GM, Amstrup S, Simac K, York G (2012) Long-distance swimming by polar bears (*ursus maritimus*) of the southern beaufort sea during years of extensive open water. Can J Zool 90:663-676

Parks EK, Derocher AE, Lunn NJ (2006) Seasonal and annual movement patterns of polar bears on the sea ice of hudson bay. Can J Zool 84:1281-1294

Pebesma EJ, Bivand RS (2005) Classes and methods for spatial data in r. R News 5:9-13

Pilfold NW, Derocher AE, Stirling I, Richardson E, Andriashek D (2012) Age and sex composition of seals killed by polar bears in the eastern beaufort sea. PLoS ONE 7:e41429

Pilfold NW, Derocher AE, Richardson E (2014a) Influence of intraspecific competition on the distribution of a wide-ranging, non-territorial carnivore. Glob Ecol Biogeogr 23:425-435

Pilfold NW, Derocher AE, Stirling I, Richardson E (2014b) Polar bear predatory behaviour reveals seascape distribution of ringed seal lairs. Popul Ecol 56:129-138

Pilfold NW, McCall A, Derocher AE, Lunn NJ, Richardson E (2017) Migratory response of polar bears to sea ice loss: To swim or not to swim. Ecography 40:189-199

Poltermann M (2001) Arctic sea ice as feeding ground for amphipods–food sources and strategies. Polar Biol 24:89-96

Potts JR, Bastille-Rousseau G, Murray DL, Schaefer JA, Lewis MA (2014) Predicting local and non-local effects of resources on animal space use using a mechanistic step selection model. Methods Ecol Evol 5:253-262

QGIS Development Team (2019) Qgis geographic information system. Open Source Geospatial Foundation Project. http://qgis.osgeo.org

R Core Team (2019) R: A language and environment for statistical computing. R Foundation for Statistical Computing, Vienna, Austria

Ramsay MA, Stirling I (1986) On the mating system of polar bears. Can J Zool 64:2142-2151

Ramsay MA, Stirling I (1988) Reproductive biology and ecology of female polar bears (*ursus maritimus*). J Zool 214:601-633

Regehr EV, Lunn NJ, Amstrup SC, Stirling I (2007) Effects of earlier sea ice breakup on survival and population size of polar bears in western hudson bay. J Wildl Manag 71:2673-2683

Regehr EV, Hunter CM, Caswell H, Amstrup SC, Stirling I (2010) Survival and breeding of polar bears in the southern beaufort sea in relation to sea ice. J Anim Ecol 79:117-127

Reimer JR, Mangel M, Derocher AE, Lewis MA (2019) Modeling optimal responses and fitness consequences in a changing arctic. Glob Change Biol 25:3450-3461

Rico A, Kindlmann P, Sedlacek F (2007) Road crossing in bank voles and yellow-necked mice. Acta Theriol (Warsz) 52:85-94

Ringuette M, Fortier L, Fortier M, Runge JA and others (2002) Advanced recruitment and accelerated population development in arctic calanoid copepods of the north water. Deep Sea Res II 49:5081-5099

Rode KD, Peacock E, Taylor M, Stirling I, Born EW, Laidre KL, Wiig Ø (2012) A tale of two polar bear populations: Ice habitat, harvest, and body condition. Popul Ecol 54:3-18

Sahanatien V, Derocher AE (2012) Monitoring sea ice habitat fragmentation for polar bear conservation. Anim Conserv 15:397-406

Sciullo L, Thiemann G, Lunn N (2016) Comparative assessment of metrics for monitoring the body condition of polar bears in western hudson bay. J Zool 300:45-58

Sciullo L, Thiemann GW, Lunn NJ, Ferguson SH (2017) Intraspecific and temporal variability in the diet composition of female polar bears in a seasonal sea ice regime. Arctic Science 3:672-688

Scott JB, Marshall GJ (2010) A step-change in the date of sea-ice breakup in western hudson bay. Arctic:155-164

Siers SR, Reed RN, Savidge JA (2016) To cross or not to cross: Modeling wildlife road crossings as a binary response variable with contextual predictors. Ecosphere 7:19

Smith M, Rigby B (1981) Distribution of polynyas in the canadian arctic. In: Stirling I, Cleator H (eds) Polynyas in the canadian arctic. Canadian Wildlife Service Occasional Paper 45, p 7-28

Smith SD, Muench RD, Pease CH (1990) Polynyas and leads: An overview of physical processes and environment. Journal of Geophysical Research: Oceans 95:9461-9479

Smith TG (1975) Ringed seals in james bay and hudson bay: Population estimates and catch statistics. Arctic:170-182

Smith TG, Stirling I (1975) The breeding habitat of the ringed seal (*phoca hispida*). The birth lair and associated structures. Can J Zool 53:1297-1305

Smith TG, Sjare B (1990) Predation of belugas and narwhals by polar bears in nearshore areas of the canadian high arctic. Arctic 43:99-102

Spreen G, Kaleschke L, Heygster G (2008) Sea ice remote sensing using amsr-e 89-ghz channels. J Geophys Res 113

Stewart DB, Barber DG (2010) The ocean-sea ice-atmosphere system of the hudson bay complex, Vol. Springer, Dordrecht

Stirling I, McEwan EH (1975) The caloric value of whole ringed seals (*phoca hispida*) in relation to polar bear (*ursus maritimus*) ecology and hunting behavior. Can J Zool 53:1021-1027

Stirling I, Archibald WR (1977) Aspects of predation of seals by polar bears. J Fish Res Board Can 34:1126-1129

Stirling I, Jonkel C, Smith P, Robertson R, Cross D (1977) The ecology of the polar bear (*ursus maritimus*) along the western coast of hudson bay, Vol 33. Minister of Supply and Services

Stirling I (1980) The biological importance of polynyas in the canadian arctic. Arctic 33:303-315

Stirling I (1981) Introduction. In: Stirling I, Cleator H (eds) Polynyas in the canadian arctic. Canadian Wildlife Service Occasional Paper 45, p 5-6

Stirling I, Cleator H, Smith TG (1981) Marine mammals. In: Stirling I, Cleator H (eds) Polynyas in the canadian arctic. Canadian Wildlife Service Occasional Paper 45, p 45-65

Stirling I, Spencer C, Andriashek D (1989) Immobilization of polar bears (*ursus maritimus*) with telazol in the canadian arctic. J Wildl Dis 25:159-168

Stirling I, Andriashek D, Calvert W (1993) Habitat preferences of polar bears in the western canadian arctic in late winter and spring. Polar Record 29:13-24

Stirling I, Derocher AE (1993) Possible impacts of climatic warming on polar bears. Arctic 46:240-245

Stirling I, Øritsland NA (1995) Relationships between estimates of ringed seal (*phoca hispida*) and polar bear (*ursus maritimus*) populations in the canadian arctic. Can J Fish Aquat Sci 52:2594-2612

Stirling I, Lunn NJ, Iacozza J (1999) Long-term trends in the population ecology of polar bears in western hudson bay in relation to climatic change. Arctic:294-306

Stirling I, Spencer C, Andriashek D (2016) Behavior and activity budgets of wild breeding polar bears (ursus maritimus). Mar Mamm Sci 32:13-37

Stroeve J, Holland MM, Meier W, Scambos T, Serreze M (2007) Arctic sea ice decline: Faster than forecast. Geophys Res Lett 34

Taylor M, Larsen T, Schweinsburg R (1985) Observations of intraspecific aggression and cannibalism in polar bears (*ursus maritimus*). Arctic:303-309

Thiemann GW, Iverson SJ, Stirling I (2008) Polar bear diets and arctic marine food webs: Insights from fatty acid analysis. Ecol Monogr 78:591-613

Thiemann GW, Iverson SJ, Stirling I, Obbard ME (2011) Individual patterns of prey selection and dietary specialization in an arctic marine carnivore. Oikos 120:1469-1478

Togunov RR, Derocher AE, Lunn NJ (2017) Windscapes and olfactory foraging in a large carnivore. Sci Rep 7:10

Togunov RR, Derocher AE, Lunn NJ (2018) Windscapes and olfactory foraging in a large carnivore (vol 7, 46332, 2017). Sci Rep 8

Tomkiewicz SM, Fuller MR, Kie JG, Bates KK (2010) Global positioning system and associated technologies in animal behaviour and ecological research. Philos Trans R Soc Lond B Biol Sci 365:2163-2176

Tremblay J-E, Gratton Y, Fauchot J, Price NM (2002) Climatic and oceanic forcing of new, net, and diatom production in the north water. Deep Sea Res II 49:4927-4946

Tschudi M, W. N. Meier, J. S. Stewart, C. Fowler, and J. Maslanik (2019) Polar pathfinder daily 25 km ease-grid sea ice motion vectors. Version 4.1. December 2009 - May 2018. Boulder, Colorado USA: National Snow and Ice Data Center. https://doi.org/10.5067/INAWUWO7QH7B. January 19, 2018

Wiig O, Derocher AE, Belikov SE (1999) Ringed seal (*phoca hispida*) breeding in the drifting pack ice of the barents sea. Mar Mamm Sci 15:595-598

APPENDIX

Table A1. Range of dates with > 95% of the Hudson Bay coastline bordered by landfast ice used to map flaw lead. Landfast ice was extracted from biweekly (January – March, 2010-2011) and weekly (March – December, 2010-2011; January-December 2012-2018) Canadian Ice Service Arctic Regional Sea Ice Charts in SIGRID-3 Format (Canadian Ice Service 2009).

Year	Start	End
2010	2009-12-21	2010-04-26
2011	2011-01-17	2011-05-16
2012	2011-12-26	2012-05-07
2013	2012-12-31	2013-05-13
2014	2013-12-16	2014-05-19
2015	2014-12-15	2015-05-04
2016	2015-12-28	2016-05-16
2017	2016-12-26	2017-05-22
2018	2017-12-25	2018-05-21

Table A2. Range and mean ± standard error of the maximum width and total area of the western Hudson Bay flaw lead (Figure 1) from December 2009 to May 2018. The western Hudson Bay flaw lead was mapped using synthetic aperture radar imagery.

Month	Maximum Width Range (km)	Mean Maximum Width (km)	Total Area Range (km^2)	Mean Total Area (km^2)
December	13.2 – 71.8	25.7 ± 2.9	281.5 – 11704.7	3837.3 ± 639.7
January	6.5 – 50.3	21.8 ± 1.2	149.3 – 11923.4	3355.2 ± 320.0
February	7.3 – 48.4	18.6 ± 1.0	517.3 – 12566.3	2380.9 ± 199.0
March	4.5 – 38.7	18.3 ± 0.8	84.1 – 7911.4	2048.4 ± 159.9
April	7.3 – 64.5	28.3 ± 1.2	181.2 – 19042.6	4290.7 ± 361.1
May	9.0 – 145.4	59.9 ± 4.9	651.2 – 30624.9	9252.1 ± 1035.3

Table A3. Akaike information criterion results for the top candidate models predicting adult female polar bear use of the flaw lead and width closest to the bear when on the flaw lead using a general linear mixed effect model. Adult female polar bears are from the Western Hudson Bay population, from January 2010 – May 2018. Individual bear identification was the random effect. January and February were pooled when width closest to the bear on the flaw lead due to small sample size (n = 10) and all points were within 26 days. k is the number of random effects terms, AIC_c is the corrected Akaike information criterion score for each model, ΔAIC_c is the difference in AIC_c scores between the top model and subsequent candidate models, w is the AIC weight, and LL is the log likelihood value. Lone (n = 12) represents a lone adult female polar bears, and COY (n = 6) represents a mother with cub(s)-of-the-year, and YRLG (n = 6) represents a mother with yearling(s). Width is the width of the flaw lead at the point closest to the bear.

Rank	Model	k	AIC_c	ΔAIC_c	w	LL
Use of Lead (n = 261)						
1	Width	3	2200	0.0	1	-1097
Width Closest to Bear (n =213)						
1	Jan/Feb + Mar + Apr + May + YRLG + COY + Lone	8	4031	0.0	1.0	- 2007
2	YRLG + COY + Lone	5	4051	20	0.0	- 2020
3	Feb + Mar + Apr + May	6	4063	32	0.0	- 2025

Table A4. Candidate models predicting adult female polar bear distance to the western Hudson Bay flaw lead and landfast ice using a linear mixed effect model. Adult female polar bears are from the Western Hudson Bay population, from December 2009 – May 2018 for the main model, and March 2010 – May 2018 for the March – May model. Individual bear identification was the random effect. COY (Main: n = 30; March – May: n = 16) represents a mother with cub(s)-of-the-year, YRLG (Main: n = 17; March – May: n = 17) represents a mother with yearling(s), and lone (Main: n = 32; March – May: n = 32) represents a lone female. Wd is the width of the flaw lead at the point closest to the bear, ar_dl is the total area and wd_dl is the maximum width of the flaw lead.

Rank	Model
Main Model (n =13505)	
1	Dec + Jan + Feb + Mar + Apr + May
2	wd_dl
3	wd_dl + wd_dl^2
4	ar
5	ar + ar^2
6	YRLG + COY + Lone
7	Dec + Jan + Feb + Mar + Apr + YRLG +COY + Lone
8	wd_dl + YRLG + COY + Lone
9	wd_dl + wd_dl^2 + YRLG + COY + Lone
10	ar + YRLG + COY + Lone
11	ar + ar^2 + YRLG + COY + Lone
March to May Only (n =10742)	

1 wd

2 $wd + wd^2$

3 wd_dl

4 $wd\_dl + wd\_dl^2$

5 ar_dl

6 $ar\_dl + ar\_dl^2$

7 wd + YRLG + COY + Lone

8 $wd\_dl + wd\_dl^2$ + YRLG + COY + Lone

9 wd_dl + YRLG + COY + Lone

10 $wd\_dl + wd\_dl^2$ + YRLG + COY + Lone

11 ar_dl + YRLG + COY + Lone

12 $ar\_dl + ar\_dl^2$ + YRLG + COY + Lone

13 YRLG + COY + Lone

Table A5. Akaike information criterion results for the top 5 candidate models predicting adult female polar bear distance to the flaw lead using a linear mixed effect model. Adult female polar bears are from the Western Hudson Bay population, from December 2009 – May 2018 for the main model, and March 2010 – May 2018 for the March – May model. Individual bear identification was the random effect. k is the number of random effects terms, AIC_c is the corrected Akaike information criterion score for each model, ΔAIC_c is the difference in AIC_c scores between the top model and subsequent candidate models, w is the AIC weight, and LL is the log likelihood value. COY (Main: n = 41; March – May: n = 20) represents a mother with cub(s)-of-the-year, YRLG (Main: n = 31; March – May: n = 31) represents a mother with yearling(s), and lone (Main: n = 42; March – May: n = 41) represents a lone female. Ar_dl is the total area and wd_dl is the maximum width of the flaw lead.

Rank	Model	k	AIC_c	ΔAIC_c	w	LL
Main Model (n =16357)						
	Dec + Jan + Feb + Mar + Apr +May +					
1	YRLG + COY + Lone	10	184376	0.0	1.0	-92178
2	Dec + Jan + Feb + Mar + Apr + May	8	184635	259	0.0	-92309
3	wd_dl + wd_dl^2 + YRLG + COY + Lone	7	185489	1114	0.0	-92738
4	wd_dl + YRLG + COY + Lone	6	185533	1157	0.0	-92760
5	ar_dl + ar_dl^2 + YRLG + COY + Lone	7	185656	1280	0.0	-92821
March to May Only (n =12895)						
1	wd_dl + wd_dl^2 + YRLG + COY + Lone	7	144483	0.0	1.0	- 72234
2	wd_dl + YRLG + COY + Lone	6	144535	53	0.0	- 72262
3	ar_dl + ar_dl^2 + YRLG + COY + Lone	7	144652	170	0.0	- 72319

4	ar_dl + YRLG + COY + Lone	6	144678	196	0.0	- 72333
5	wd_dl + wd_dl^2	5	144688	205	0.0	- 72339

Table A6. Akaike information criterion results for the top 5 candidate models predicting adult female polar bear distance to western Hudson Bay landfast ice using a linear mixed effect model. Adult female polar bears are from the Western Hudson Bay population, from December 2009 – May 2018 for the main model, and March 2010 – May 2018 for the March – May model. Individual bear identification was the random effect. k is the number of random effects terms, AIC_c is the corrected Akaike information criterion score for each model, ΔAIC_c is the difference in AIC_c scores between the top model and subsequent candidate models, w is the AIC weight, and LL is the log likelihood value. COY (Main: n = 41; March – May: n = 20) represents a mother with cub(s)-of-the-year, YRLG (Main: n = 31; March – May: n = 31) represents a mother with yearling(s), and lone (Main: n = 42; March – May: n = 41) represents a lone female. Wd is the width of the flaw lead at the point closest to the bear, ar_dl is the total area and wd_dl is the maximum width of the flaw lead.

Rank	Model	k	AIC_c	ΔAIC_c	w	LL
Main Model (n =16357)						
1	Dec + Jan + Feb + Mar + Apr + May + YRLG + COY	10	183938	0.0	1.0	- 91959
2	Dec + Jan + Feb + Mar + Apr + May	8	184157	219	0.0	- 92071
3	wd_dl + YRLG + COY + Lone	6	185446	1508	0.0	-92717
4	$wd\_dl + wd\_dl^2$ + YRLG + COY + Lone	7	185447	1509	0.0	- 92717
5	ar + ar^2 + YRLG +COY + Lone	7	185579	1641	0.0	- 92782
March to May Only (n =12895)						
1	wd_dl + YRLG + COY + Lone	6	144137	0.0	0.7	- 72062

	wd_dl + wd_dl^2 + YRLG + COY +					
2	Lone	7	144139	2	0.3	- 72062
3	ar_dl + ar_dl^2 + YRLG + COY + Lone	7	144264	128	0.0	- 72125
4	ar_dl + YRLG + COY + Lone	6	144284	148	0.0	- 72136
5	wd_dl	4	144297	161	0.0	- 72144

Table A7. Covariate coefficient estimates for the top models predicting adult female polar bear distance to the western Hudson Bay landfast ice using a maximum likelihood linear mixed effects model. Adult female polar bears are from the Western Hudson Bay polar bear population from December 2009 – May 2018 for the main model, and March 2010 – May 2018 for the March to May model ($\alpha = 0.05$). YRLG represents a mother with yearling(s), and COY represents a mother with cub(s)-of-the-year. Daily max width is the maximum width of the flaw lead on the date of the polar bear location.

				95% CI		
Model	Parameter	Estimate	SE	Lower	Upper	*p* value
Main Model	December	162.1	3.9	154.4	169.7	<0.001
	January	83.0	2.6	77.9	88.1	<0.001
	February	49.2	2.6	44.1	54.2	<0.001
	March	34.0	1.6	30.8	37.2	<0.001
	April	38.8	1.6	35.8	41.9	<0.001
	YRLG	-20.8	1.7	-24.1	-17.4	<0.001
	COY	-20.0	1.7	-23.2	-16.7	<0.001
	Constant	156.2	10.5	135.7	176.7	<0.001
March to	Daily Max Width	3.7E-05	1.9E-05	4.1E-07	7.4E-05	<0.001
May	YRLG	-12.0	2.0	-15.9	-8.1	<0.001
	COY	-21.2	1.8	-24.8	-17.6	<0.001
	Constant	170.1	13.6	143.5	196.7	<0.001

Table A8: Log likelihood ratio results of the best fit von Mises model for the adult female polar bear movements relative to the western Hudson Bay flaw lead and turning angles from December 2009 – May 2018. Adult female polar bears are from the Western Hudson Bay polar bear population from December 2009 – May 2018 . μ is the mean of the peak and k is the kappa. The bolded μ is the most prominent peak. Relative movement directions were divided into 3 groups: towards ($-45° \leq \theta \leq 45°$), along ($-45° > \theta > -135°$) and ($45° < \theta < 135°$), and away ($-135° \leq \theta \geq 135°$) from the flaw lead. Turning angles were divided into 3 groups: low ($-45° \leq \theta \leq 45°$), turn ($-45° > \theta > -135°$ & $45° < \theta < 135°$), and reversal turn ($-135° \leq \theta \geq 135°$; $\alpha = 0.05$).

		μ_1	k_1	μ_2	k_2	Prominent Move Angle	χ^2	df	*p* value
Movement Relative to the Flaw Lead	On	**101**	4.7	-69	0.2	Along	11	5	<0.05
	Near	160	0.3	**-23**	4.4	Towards	21	5	<0.01
	Off	149	1.4	**-31**	1.9	Towards	2189	5	<0.001
	December	**150**	3.0	-40	0.8	Away	256	5	<0.001
	January	154	1.4	**-28**	2.3	Towards	556	5	<0.001
	February	**147**	1.3	-34	1.8	Away	309	5	<0.001
	March	147	1.1	**-35**	2.1	Towards	438	5	<0.001
	April	149	1.3	**-26**	1.8	Towards	492	5	<0.001
	May	147	1.1	**-31**	1.9	Towards	259	5	<0.001
Turning Angles	On	**16**	3.0	-142	0.5	Low	52	5	<0.001
	Near	**65**	0.5	NA	NA	90 Deg	123	2	<0.001
	Off	**29**	1.1	-20	0	Low	2873	5	<0.001
	December	**7**	2.0	-112	0	Low	2642	5	<0.001

January	**20**	1.4	-24	0.0	Low	1721	5	<0.001
February	**38**	0.6	NA	NA	Low	959	2	<0.001
March	**33**	0.7	NA	NA	Low	1637	2	<0.001
April	**36**	0.6	NA	NA	Low	1457	2	<0.001
May	**39**	0.6	NA	NA	Low	1220	2	<0.001

Table A9: Comparison of 4 different spatial scales for estimating even interval tracks to calculate the radius of peak variance in $\log_{10}$-transformed first passage time of adult female polar bears using a Spearman's rank correlation coefficient. Five tracks from two adult female polar bears from the Western Hudson Bay population were used ($\alpha = 0.05$).

	2 km		1 km		5 km	
	r	*p* value	r	*p* value	r	*p* value
3.3 km	0.95	<0.001	0.92	<0.001	0.93	<0.001
2 km			0.98	<0.001	0.87	<0.001
1 km					0.84	<0.001

Table A10. Candidate models predicting adult female polar bear log_{10}-transformed first passage time using a linear mixed effect model. Adult female polar bears are from the Western Hudson Bay population, from December 2009 – May 2018 for the main model, March 2010 – May 2018 for the March – May model, and January 2010 – May 2018 for the on the flaw lead model. Individual bear identification was the random effect. January and February were pooled when predicting first passage time on the flaw lead due to small sample size (n = 5), and all points were within 26 days. COY (Main: n = 29; March – May: n = 16; On: n = 5) represents a mother with cub(s)-of-the-year, YRLG (Main: n = 17; March – May: n = 17; On: n = 4) represents a mother with yearling(s), and lone represents a lone female (Main: n = 32; March – May: n = 32; On: n = 10). wd is the width of the flaw lead at the point closest to the bear, ar_dl is the total area and wd_dl is the maximum width of the flaw lead.

Rank	Model
Main Model (n =13505)	
1	Dec + Jan + Feb + Mar + Apr + May
2	dist_ld
3	dist_ld + $dist\_ld^2$
4	Dec + Jan + Feb + Mar + Apr + May + YRLG + COY + Lone
5	YRLG + COY + Lone
March to May Only (n =10742)	
1	wd
2	wd + wd^2
3	wd_dl
4	wd_dl + wd_dl^2

5 ar_dl

6 ar_dl + ar_dl^2

7 wd + YRLG + COY

8 wd_dl + wd_dl^2 + YRLG + COY + Lone

9 wd_dl + YRLG + COY + Lone

10 wd_dl + wd_dl^2 + YRLG + COY + Lone

11 ar_dl + YRLG + COY

12 ar_dl + ar_dl^2 + YRLG + COY + Lone

13 YRLG + COY + Lone

On the Flaw Lead (n =128)

1 dist_ld

2 dist_ld + $dist\_ld^2$

3 wd

4 wd + wd^2

5 dist_ld + wd

6 dist_ld + $dist\_ld^2$ + wd + wd^2

7 dist_ld + wd + wd^2

8 dist_ld + $dist\_ld^2$ + wd

9 Jan/Feb + Mar + Apr + May

10 Jan/Feb + Mar + Apr + May + wd

11 Jan/Feb + Mar + Apr + May + wd + wd^2

12 Jan/Feb + Mar + Apr + May + YRLG + COY + Lone

13 YRLG + COY + Lone

Table A11. Akaike information criterion results for the top 5 candidate predicting female polar bear log_{10}-transformed first passage time using a linear mixed effect model. Female polar bears are from the Western Hudson Bay population, from December 2009 – May 2018, March 2010 – May 2018 for the March – May model, and January 2010 – May 2018 for the on the flaw lead model. Individual bear identification was the random effect. January and February were pooled when predicting first passage time on the flaw lead due to small sample size (n = 5), and all points were within 26 days. k is the number of fixed effect terms, AIC_c is the corrected Akaike information criterion score for each model, ΔAIC_c is the difference in AIC_c scores between the top model and subsequent candidate models, w is the AIC weight, and LL is the log likelihood value. COY (Main: n = 29; March – May: n = 16; On: n = 5) represents a mother with cub(s)-of-the-year, YRLG (Main: n = 17; March – May: n = 17; On: n = 4) represents a mother with yearling(s), and lone represents a lone female (Main: n = 32; March – May: n = 32; On: n = 10). Dist_ld is the bears distance to the nearest point of the flaw lead, wd is the width of the flaw lead at the point the bear is closest to.

Rank	Model	k	AIC_c	ΔAIC_c	w	LL
Main Model (n =9018)						
1	Dec + Jan + Feb + Mar + Apr + May + COY + YRLG + Lone	10	16692	0.0	1.0	-8336
2	COY + YRLG + Lone	5	16766	73	0.0	-8378
3	Dec + Jan + Feb + Mar + Apr + May	8	16769	76	0.0	-8377
4	dist_ld	4	16797	104	0.0	-8394
5	dist_ld + $dist\_ld^2$	5	16799	106	0.0	-8394
March to May Only (n =7252)						

1	dist_ld	4	13405	0.0	0.4	-6699
2	dist_ld + wd	5	13406	1.4	0.2	-6698
3	dist_ld + $dist\_ld^2$	5	13407	1.5	0.1	-6698
4	dist_ld + wd + wd^2	6	13407	2.0	0.1	-6697
5	dist_ld + $dist\_ld^2$ + wd	6	13408	2.8	0.1	-6698
On the Flaw Lead (n =128)						
1	wd	4	202.2	0.00	0.4	-97
2	Jan/Feb + Mar + Apr + May + wd	7	203.9	1.7	0.2	-94
3	wd + dist_ld	5	204.0	1.9	0.2	-97
4	wd + wd^2	5	204.3	2.1	0.1	-97
5	wd + dist_ld + $dist\_ld^2$	6	206.1	3.9	0.1	-97

Table A12. Adult female polar bear trips on the western Hudson Bay flaw lead from January 2010 – May 2018. Adult female polar bears are from the Western Hudson Bay population. Bear ID is the individual bear identification, and RS is the bear reproductive status. Lone represents a lone female, COY represents a mother with cub(s)-of-the-year, YRLG represents a mother with yearling(s), and UNK the reproductive status is unknown. Arrive and leave are the date and time of the first location and last location of the polar bear on the flaw lead for each trip respectively. Cross start is the date and time of the last location before the bear started crossing the flaw lead, and cross end is the date and time of the first location on the other side of the flaw lead. Mean area and mean width are the mean values over the trip on the flaw lead. NA indicates bear did not cross the flaw lead.

Bear ID	RS	Arrive	Leave	Cross Start	Cross End	Mean Area (km^2)	Mean Width (km)	Cross Start Width (km)
X03486	Lone	2010-04-25 9:00	2010-04-25 13:00	2010-04-25 13:00	2010-04-25 17:00	0.73	1.14	0.25
X12208	UNK	2010-01-29 1:00*	2010-02-01 5:00	2010-01-31 13:00	2010-02-01 9:00	6861.08	12.30	10.02
X12627	Lone	2015-04-25 5:00*	2015-04-25 5:00	NA	NA	1.69	1.00	NA
X17097	UNK	2010-03-11 1:00*	2010-03-11 21:00	NA	NA	2319.30	7.78	NA
X17097	UNK	2010-03-13 9:00	2010-03-14 17:00	NA	NA	666.86	8.25	NA

X17339	Lone	2016-04-03 1:00	2016-04-03 13:00	2016-04-03 1:00	2016-04-03 13:00	1.58	2.09	2.78
X17598	UNK	2018-04-14 1:00	2018-04-14 13:00	NA	NA	93.78	2.15	NA
X17598	UNK	2018-04-20 1:00	2018-04-22 9:00	NA	NA	535.73	15.27	NA
X17598	UNK	2018-04-23 21:00	2018-04-24 21:00	NA	NA	535.73	19.54	NA
X17598	UNK	2018-05-14 17:00	2018-05-15 21:00	NA	NA	1.51	3.96	NA
X19143	COY	2017-03-06 17:00**	2017-03-06 21:00	2017-03-06 21:00	2017-03-07 1:00	0.34	0.46	0.46
X19143	YRLG	2018-04-06 3:00	2018-04-07 11:00	2018-04-07 3:00	2018-04-07 11:00	4.53	1.67	NA
X19295	COY	2014-03-07 1:00	2014-03-10 13:00	2014-03-10 5:00	2014-03-10 13:00	17.51	2.52	3.71
X19389	COY	2016-03-31 1:00	2016-04-02 17:00	2016-04-01 17:00	2016-04-02 1:00	206.76	8.94	5.16
X19602	Lone	2011-04-13 5:00	2011-04-13 21:00	NA	NA	1375.82	10.70	NA
X19602	Lone	2011-04-17 1:00***	2011-04-18 13:00	2011-04-18 1:00	2011-04-18 13:00	5758.14	12.71	10.80
X19602	Lone	2011-04-18 13:00***	2011-04-20 13:00	2011-04-19 21:00	2011-04-20 9:00	533.50	7.02	3.71
X19602	Lone	2011-04-26 5:00	2011-04-26 21:00	NA	NA	813.40	11.72	NA

X19602	Lone	2011-05-08 1:00	2011-05-10 21:00	2011-05-08 21:00	2011-05-10 21:00	2.52	30.33	1.57
X19602	Lone	2011-05-14 21:00	2011-05-16 17:00	2011-05-16 9:00	2011-05-16 17:00	0.96	0.82	0.81
X19602	COY	2012-03-24 5:00	2012-03-24 9:00	2012-03-24 5:00	2012-03-24 9:00	0.86	1.12	1.12
X19627	Lone	2015-05-02 13:00	2015-05-04 5:00	2015-05-03 9:00	2015-05-04 9:00	995.22	14.14	14.52
X19654	COY	2013-03-26 1:00**	2013-03-26 17:00	2013-03-26 9:00	2013-03-26 17:00	2.86	2.64	2.88
X19826	YRLG	2015-04-23 9:00	2015-04-27 21:00	NA	NA	102.57	4.58	NA
X19939	YRLG	2016-05-15 9:00	2016-05-16 5:00	NA	NA	21062.68	113.28	NA
X19939	Lone	2017-05-12 1:00	2017-05-13 1:00	NA	NA	2355.71	6.19	NA
X19939	Lone	2017-05-21 1:00	2017-05-21 21:00	NA	NA	3891.67	18.52	NA
X32491	Lone	2011-02-11 17:00	2011-02-11 17:00	NA	NA	1.30	0.84	NA
X33228	YRLG	2018-05-11 17:00	2018-05-11 17:00	2018-05-11 13:00	2018-05-11 17:00	1.27	1.52	1.45
X33228	YRLG	2018-05-15 17:00	2018-05-15 17:00	NA	NA	1.41	1.69	NA
X33326	Lone	2010-04-18 17:00	2010-04-19 21:00	NA	NA	3336.62	48.25	NA
X33410	Lone	2016-05-03 17:00***	2016-05-03 21:00	2016-05-03 17:00	2016-05-03 21:00	2.23	1.16	0.82

X33410	Lone	2016-05-03 21:00***	2016-05-04 1:00	2016-05-04 1:00	2016-05-04 5:00	2.23	1.55	1.75
X33412	Lone	2017-05-14 1:00	2017-05-14 21:00	2017-05-14 1:00	2017-05-14 5:00	0.45	2.17	1.03
X33412	Lone	2017-05-16 17:00	2017-05-16 17:00	2017-05-16 17:00	2017-05-16 21:00	1.08	1.27	0.91
X33412	Lone	2018-01-20 1:00	2018-01-20 21:00	2018-01-20 13:00	2018-01-20 17:00	19.90	2.82	2.79
X33510	COY	2014-03-07 9:00**	2014-03-08 1:00	2014-03-07 13:00	2014-03-07 17:00	301.56	10.82	6.17
X33510	YRLG	2015-03-10 5:00**	2015-03-10 9:00	2015-03-10 5:00	2015-03-10 9:00	1.51	0.90	0.90
X33563	YRLG	2014-04-13 9:00	2014-04-13 21:00	NA	NA	77.72	9.11	NA
X33563	YRLG	2014-05-02 5:00	2014-05-02 5:00	NA	NA	2.83	1.88	NA
X33563	Lone	2015-04-16 1:00	2015-04-16 21:00	NA	NA	1.10	1.11	NA
X33563	Lone	2015-05-02 1:00	2015-05-02 13:00	NA	NA	4.40	1.94	NA
X33563	Lone	2016-02-15 13:00	2016-02-15 21:00	2016-02-15 13:00	2016-02-15 21:00	193.63	2.63	3.34
X33579	UNK	2018-04-27 9:00	2018-04-28 21:00	NA	NA	3.20	3.10	NA
X33693	Lone	2018-05-08 13:00	2018-05-08 21:00	NA	NA	1.33	3.30	NA

X33693	Lone	2018-05-11 1:00	2018-05-15 1:00	NA	NA	3.48	1.95	NA

*Bear was already on the flaw lead when SAR Imagery was available.

**Bear was returning to ice from land.

***Bear crossed the flaw lead twice before end of trip.

Table A13. Candidate models predicting adult female polar bear crossing of the western Hudson Bay flaw lead using a generalized linear mixed effect model. Adult female polar bears are from the Western Hudson Bay population, from January 2010 – May 2018. January (n = 2), February (n = 2), and March (n = 9) were pooled because of small sample size, and the width of the flaw lead did not significantly differ in these months. Individual bear identification was the random effect. End Width is the width of the flaw lead when the bear begins crossing, or when the bear leaves the flaw lead without crossing, start width is the width of the flaw lead for the bear's first location on the flaw lead, and mean width is the mean width of the flaw lead for the bear's trip on the flaw lead.

Rank	Model
Crossing Rate (n =46)	
1	End Width
2	End Width + End Width ^{2}
3	Jan-Mar + Apr + May
4	Jan-Mar + Apr + May + End Width
5	Jan-Mar + Apr + May + End Width + End Width ^{2}
6	Start Width
7	Start Width + Start Width^2
8	Jan-Mar + Apr + May + Start Width
9	Jan-Mar + Apr + May + Start Width + Start Width ^{2}
10	Mean Width
11	Mean Width + Mean Width^2

12	Jan-Mar + Apr + May + Mean Width
13	Jan-Mar + Apr + May + Mean Width + Mean Width ^{2}

Table A14. Akaike information criterion results for top 5 candidate models predicting adult female polar bear crossing of the western Hudson Bay flaw lead using a generalized linear mixed effect model. Adult female polar bears are from the Western Hudson Bay population, from January 2010 – May 2018. January (n = 2), February (n = 2), and March (n = 9) were pooled because of small sample size, and the width of the flaw lead did not significantly differ in these months. Individual bear identification was the random effect. k is the number of fixed effect terms, AIC_c is the corrected Akaike information criterion score for each model, ΔAIC_c is the difference in AIC_c scores between the top model and subsequent candidate models, w is the AIC weight, and LL is the log likelihood value. End width is the width of the flaw lead when the bear begins crossing, or when the bear leaves the flaw lead without crossing, and start width is the width of the flaw lead for the bear's first location on the flaw lead.

Rank	Model	k	AIC_c	ΔAIC_c	w	LL
Crossing Rate (n =46)						
1	Jan-Mar + April + May + End Width	5	54.7	0.00	0.32	-21.6
2	Jan-Mar + April + May	4	55.2	0.47	0.25	-23.1
3	Jan-Mar + April + May + End Width + End Width ^{2}	6	57.3	2.61	0.09	-21.6
4	End Width	3	57.4	2.73	0.08	-25.4
5	Jan-Mar + April + May + Start Width	5	57.5	2.83	0.08	-23.0

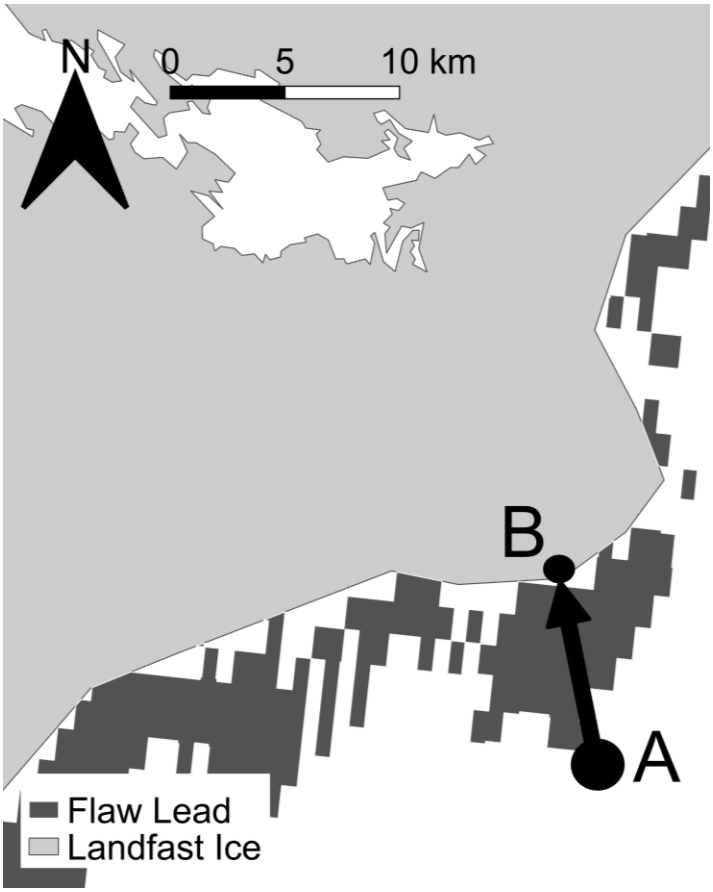

Figure A1: Example of calculating the width of the western Hudson Bay flaw lead polynya. The maximum width was calculated as the straight-line distance from the edge of the flaw lead (A) to the closest point on the landfast ice (B). The flaw lead was mapped using synthetic aperture radar imagery from December 2009 – May 2018. Landfast ice was extracted from the Canadian Ice Service Arctic Regional Sea Ice Charts in SIGRID-3 Format. Weekly sea ice charts were available for the whole period except January – March of 2010 – 2011, when biweekly sea ice charts were used. The width closest to the Western Hudson Bay adult female polar bears position was calculated in the same manner. Adult female polar bears are from the Western Hudson Bay population, from December 2009 – May 2018.

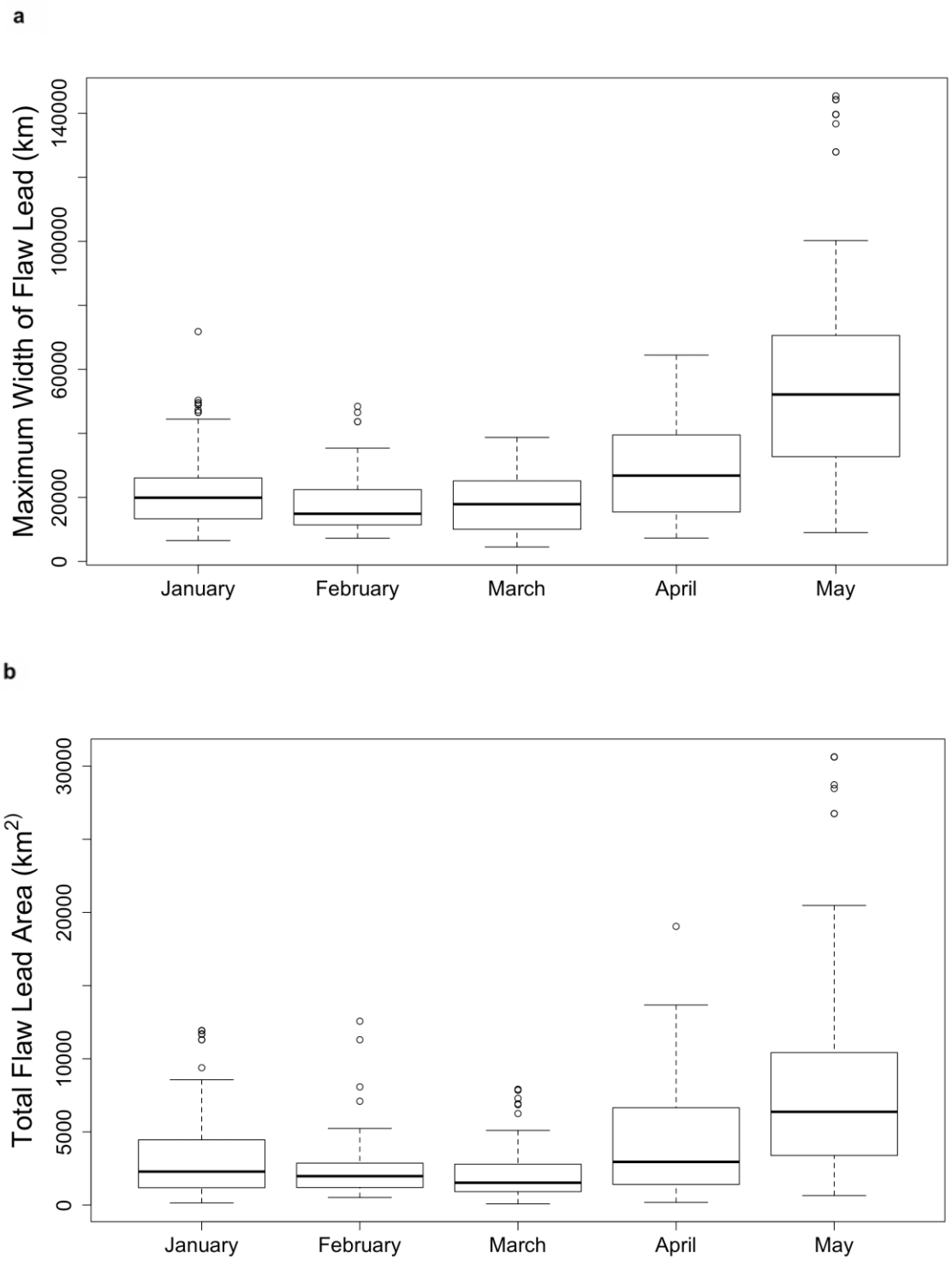

Figure A2. Comparison of the western Hudson Bay flaw lead (a) maximum width (km) and (b) total area (km^2) by month from December 2009 – May 2018. The flaw lead was mapped using synthetic aperture radar. December and January were compared using a Wilcoxon signed-rank

test ($\alpha = 0.05$) and determined to not significantly differ in maximum width (Wilcoxon signed-rank $z = -0.05$, $p = 0.96$), or total area (Wilcoxon signed-rank $z = -0.88$, $p = 0.37$), therefore these months were pooled due to small sample size in December ($n = 23$), and to account for the time period of December being less than two weeks.

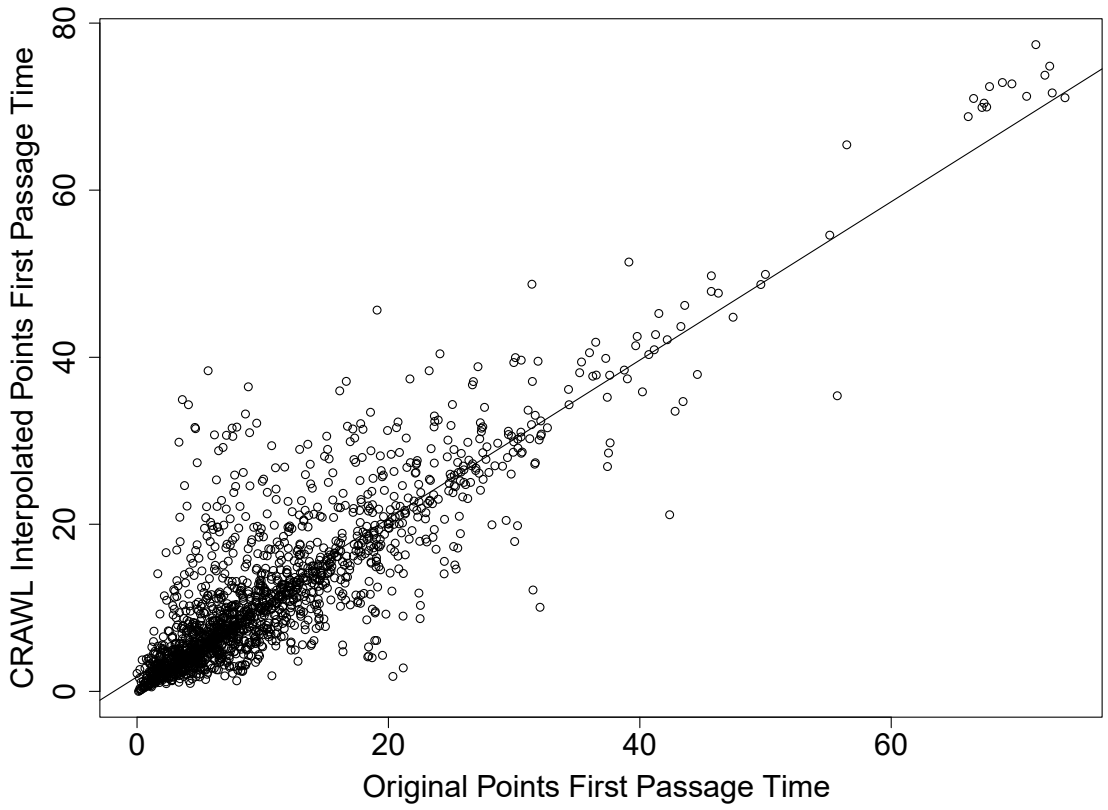

Figure A3: Comparing first passage time calculated from adult female polar bear original locations to first passage time calculated from locations where 50% of the adult female polar bear's track was interpolated using CRAWL. Five tracks from two adult female polar bears from the Western Hudson Bay population were used. Spearman's rank $r = 0.82$, $p < 0.001$ ($\alpha = 0.05$).

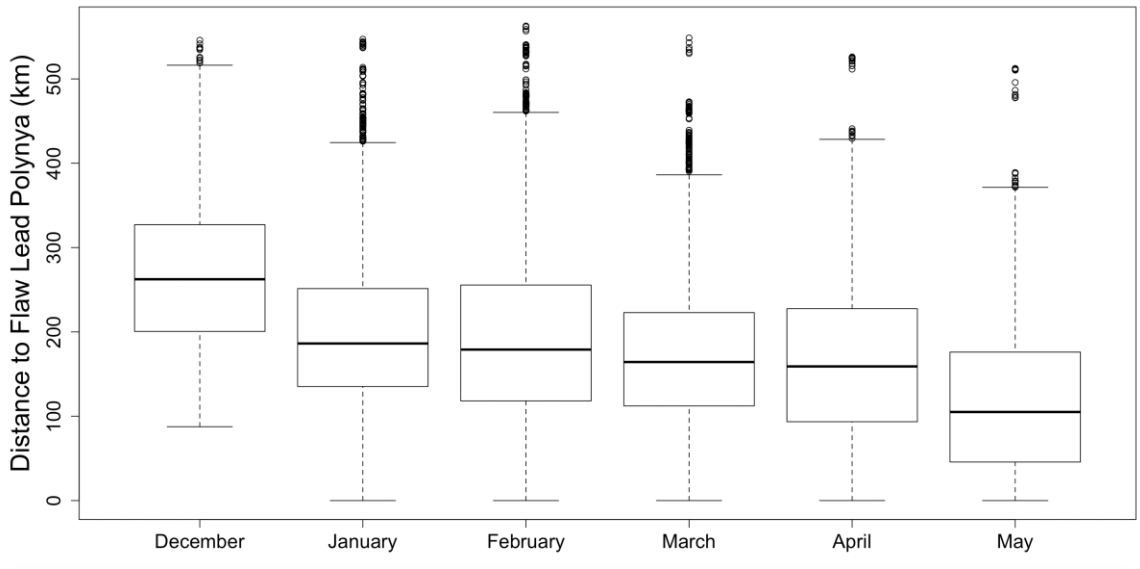

Figure A4. Adult female polar bears distance (km) to the western Hudson Bay flaw lead by month from December 2009 – May 2018. Adult female polar bears are from the Western Hudson Bay population. The flaw lead was mapped using synthetic aperture radar.

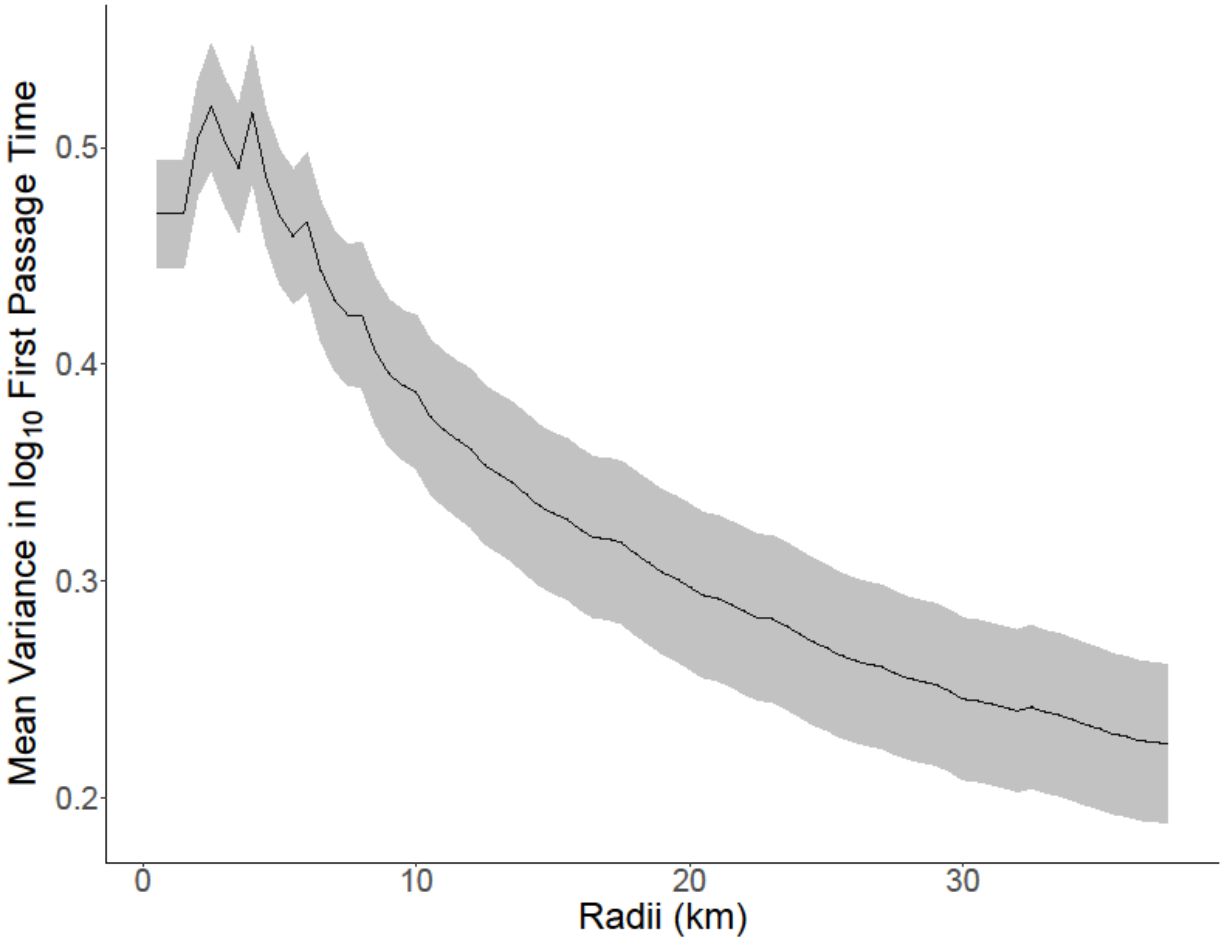

Figure A5: Mean variance in $\log_{10}$-transformed first passage time with 95% CI for all western Hudson Bay adult female polar bears from December 2009 – May 2018. First passage time is the amount of time for the bear to cross a circle of a given radius. Peak variance in $\log_{10}$-transformed first passage time is the spatial scale at which the bear undergoes area restricted search. Peak variance occurred for all tracks for all bears at a radius of 2.5 km.

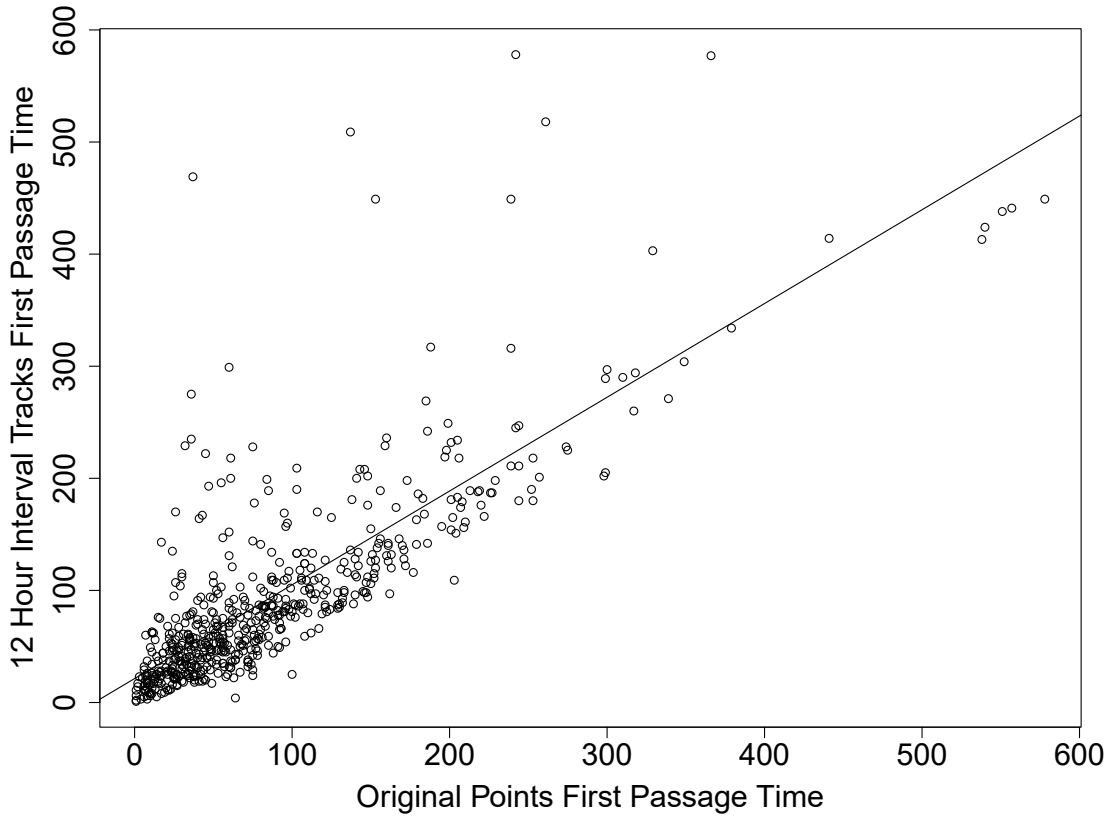

Figure A6: Comparing first passage time calculated using adult female polar bear locations separated by 4 hour intervals to first passage time calculated using adult female polar bear locations separated by 12 hour intervals. Five tracks from two female polar bears from the Western Hudson Bay population were used. Spearman's rank $r = 0.80$, $p < 0.001$ ($\alpha = 0.05$).